TECHNISCHE
UNIVERSITÄT
DARMSTADT

Fachbereich Physik
Institut für Kernphysik · Theoriezentrum

Dyson–Schwinger Approach to the Taylor Coefficients of the Quark Pressure

Dyson–Schwinger-Zugang zu den Taylor-Koeffizienten des Quark-Drucks

Master's Thesis

Philipp Isserstedt

February 2017
(Corrections: April 2017)

Supervision:
Priv.-Doz. Dr. Michael Buballa

Dyson–Schwinger Approach to the Taylor Coefficients of the Quark Pressure
Dyson–Schwinger-Zugang zu den Taylor-Koeffizienten des Quark-Drucks

Dem Fachbereich Physik der Technischen Universität Darmstadt
vorgelegte Master-Arbeit von Philipp Isserstedt, B.Sc.

1. Gutachten: Priv.-Doz. Dr. Michael Buballa
2. Gutachten: Prof. Dr. Christian Fischer (Justus-Liebig-Universität Gießen)

Tag der Einreichung: 22. Februar 2017
Korrigierte Version: 3. April 2017

Abstract

We study the Taylor coefficients of the quark pressure with respect to the chemical potential μ about $\mu = 0$ with Dyson–Schwinger equations. The Dyson–Schwinger equation for the dressed (i.e. nonperturbative) quark propagator is solved in the vacuum as well as at nonzero temperature and chemical potential within a rainbow-ladder truncation. Furthermore, we derive and solve self-consistent equations determining the derivatives of the dressed quark propagator with respect to μ at $\mu = 0$. Finally, we investigate the first three Taylor coefficients of the quark pressure.

Zusammenfassung

Wir untersuchen die Taylor-Koeffizienten des Quark-Drucks bezüglich des chemischen Potentials μ um $\mu = 0$ mittels Dyson–Schwinger-Gleichungen. Die Dyson–Schwinger-Gleichung für den gedressten (d.h. nicht-störungstheoretischen) Quark-Propagator wird im Vakuum und bei nicht verschwindender Temperatur und nicht verschwindenden chemischen Potential gelöst. Weiterhin leiten wir selbstkonsistente Gleichungen für die Ableitungen des gedressten Quark-Propagators nach μ und ausgewertet bei $\mu = 0$ her und lösen diese. Am Ende untersuchen wir die ersten drei Taylor-Koeffizienten des Quark-Drucks.

Contents

1. Introduction

Up to the late 1960's, the vast amount of elementary particles discovered by experimental particle physicists were believed to be literally elementary, i.e. having no substructure. This also included the building blocks of atomic nuclei, the proton and the neutron. Aiming an explanation of this so-called "particle zoo" led to the proposition by Gell-Mann and Zweig in 1964 [1, 2] that these particles are not elementary but consist of quarks, held together by the so-called strong force. This idea was supported by the first high-energy electron-proton scattering experiments, indicating for the first time that the proton contains smaller point-like objects [3, 4]. Almost one decade after the proposition of quarks, a theory called quantum chromodynamics (QCD) was introduced [5, 6]. It contains quarks as fundamental constituents and gluons, which mediate the strong force. The latter interact with the quarks as well as among themselves, making QCD non-abelian and thus distinct from quantum electrodynamics, the field theory of electrons and photons. One of the most important features of QCD is asymptotic freedom, which describes the behaviour that the higher the energy the smaller the coupling of quarks and gluons. This remarkable fact was shown by Gross and Wilczek [7] and independently by Politzer [8]. The experimental confirmation (see Ref. [9] for an overview) led to the wide acceptance of QCD as the theory describing the strong interaction. Another interesting feature of QCD is confinement, stating that in the low-energy region, quarks and gluons only appear in bound states and are not observed freely, which is not yet completely understood.

Of particular interest is the phase diagram of QCD [10, 11], where T denotes the temperature and μ the quark chemical potential. A sketch is shown in Figure 1.1.

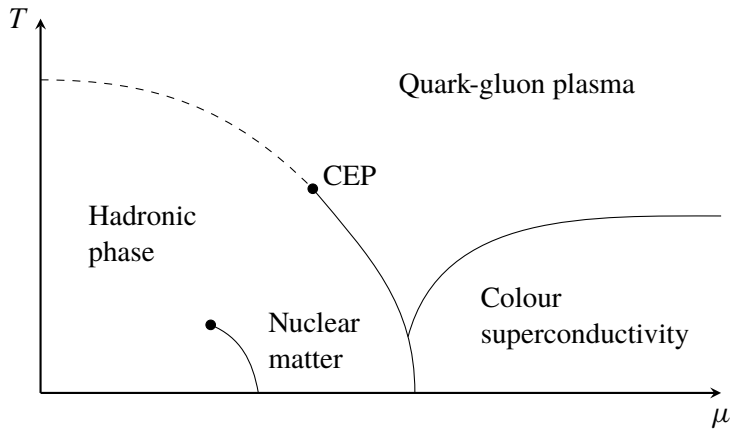

Figure 1.1.: Sketch of the QCD phase diagram in the (T, μ)-plane.

In the domain of low temperature and density, we are in the hadronic phase where quarks and gluons are confined to hadrons and chiral symmetry is broken. The region of $T \approx 0$ and small chemical potential corresponds to the vacuum. For higher quark chemical potentials one crosses a first-order phase boundary characterising the gas-liquid phase transition to nuclear matter. For even higher μ, colour-superconducting phases occur. Similar to the gas-liquid transition, a first order phase transition separates the quark-gluon plasma where quarks and gluons are deconfined and chiral symmetry is restored, from the hadronic phase for intermediate temperature and chemical potential. This transition terminates in a critical endpoint (CEP) where the transition is of second order. From there on, for smaller quark chemical potential, the transition becomes a crossover (dashed line in Figure 1.1). Another phase that might appear, although not indicated in Figure 1.1, is an inhomogeneous one at intermediate temperature and density.

However, the phase diagram of quantum chromodynamics described as above is mostly conjectured and its true realisation is subject to many experimental and theoretical efforts (see e.g. [12] for an overview). From a theoretical point of view, different tools are needed to explore the various domains of the phase diagram. First of all, due to the complexity of QCD, an often used approach is an effective theory which is based on QCD but accompanied with certain simplifications. A prominent example is the Nambu–Jona-Lasinio model [13, 14], where the gluons are infinitely heavy resulting in an effective four-quark interaction. It was successfully applied to investigate colour-superconductivity and inhomogeneous phases, see e.g. [15, 16] for a review. A second approach is the use of functional methods, namely the Dyson–Schwinger equations (DSEs) [17–19] and the functional renormalisation group [20]. The latter deals with differential equations of correlation functions with respect to an auxiliary infrared scale and applications concerning the phase diagram can be found, for example, in [21, 22]. The DSEs on the other hand are coupled integral equations of the correlation functions. They had proven to be a powerful tool accessing different regions of the phase diagram. Selected results can be found in Refs. [23–28]. A third method is lattice QCD, an ab-initio approach which discretises the theory on a finite space-time grid. Due to that, the former infinite-dimensional path integral becomes finite-dimensional and can be computed via Monte-Carlo methods. While well-established results for vanishing quark chemical potential are obtained, lattice QCD has a conceptual problem if one tries to calculate at $\mu \neq 0$. The reason is that the fermion determinant used as a probability measure for the Monte-Carlo algorithm becomes complex. This is known as the "sign problem". Despite much effort (see e.g. [29–31]), the sign problem has not been resolved completely yet. A rather straightforward way to obtain insights at nonvanishing chemical potential from lattice QCD is a Taylor expansion of quantities with respect to μ about $\mu = 0$. This expansion can be used to extrapolate to $\mu \neq 0$.

The present work is concerned with the aforementioned Taylor expansion technique. Our aim is to calculate the Taylor coefficients of the quark pressure with respect to μ about $\mu = 0$ using Dyson–Schwinger equations. This has been done in the Nambu–Jona-Lasinio model as well as on the lattice, but to our knowledge never from a Dyson–Schwinger perspective. Such a study can be used as another test for the Dyson–Schwinger equations as an nonperturbative approach to QCD by comparing the results with lattice QCD. Another possibility is the investigation of the radius of convergence of the Taylor expansion with respect to μ about $\mu = 0$.

The document is organised as follows: In the next chapter we discuss the essential aspects of QCD and derive the DSE for the fully dressed (i.e. nonperturbative) quark propagator in vacuum (defined by $T = \mu = 0$) as well as at nonzero temperature and quark chemical potential. How to truncate and solve the DSE for the quark propagator is the subject of Chapter 3. The subsequent fourth chapter makes contact to thermodynamics and we present our results regarding the Taylor coefficients of the quark pressure. We close with a summary of the work which has been done and give a short outlook of possible future research.

2. Theoretical Framework

2.1. Quantum Chromodynamics

In the following we try to summarise the concept and formalism of QCD. Since a comprehensive treatment is beyond the scope of this section, we refer to the textbooks [32–35], on which the following is based on.

2.1.1. Basic Setup

QCD is the quantum field theory describing the strong interaction. It is a non-abelian gauge theory constrained by locality, Poincaré-invariance, local gauge invariance, and renormalisability. The fundamental constituents of QCD are spin-$\frac{1}{2}$ Dirac spinors, called quarks, and spin-1 gauge bosons, the gluons, which interact with the quarks and among themselves. The quarks occur in $N_\mathrm{f} = 6$ different types, called flavours, namely up, down, strange, charm, bottom, and top. Furthermore, each quark flavour carries an additional degree of freedom, called colour, where the number of colours is $N_\mathrm{c} = 3$ (referred to as red, green, and blue).

As in every field theory, QCD is described by a Lagrangian. The gauge group is the non-abelian group $\mathrm{SU}(N_\mathrm{c})$ and the quarks belong by construction to the fundamental representation of it. The QCD Lagrangian can be obtained from the free field Lagrangian by imposing the beforehand mentioned principle of local gauge invariance. Since different quark flavours enter the Lagrangian additively, we consider only one flavour for simplicity. The quark Lagrangian reads [1]

$$\mathscr{L}_\mathrm{quark} := \bar{\psi}\left(-\not{\partial} + m\right)\psi \tag{2.1}$$

where ψ denotes the quark field, $\bar{\psi} := \psi^\dagger\gamma_4$ its Dirac adjoint, and m is the unrenormalised (bare) quark mass. We supressed colour and Dirac indices, i.e. ψ is an N_c-component vector in colour space whose components are Dirac spinors. Local gauge invariance now means that $\mathscr{L}_\mathrm{quark}$ is invariant under the transformation $\psi \to \psi' := U\psi$, where $U \in \mathrm{SU}(N_\mathrm{c})$ is spacetime-dependent. The mass term in (2.1) is obviously invariant while the derivative generates a term containing $\partial_\mu U$, which prevents the invariance [2]. To overcome this problem, the usual derivative is replaced with a covariant one:

$$\partial_\mu \to D_\mu := \partial_\mu + \mathrm{i}g_\mathrm{s}A_\mu^a T^a \ , \tag{2.2}$$

[1] We refer to Appendix A for our notations and conventions. Most notably, we work solely in Euclidean spacetime.

[2] For a global (i.e. spacetime-independent) transformation, (2.1) is obviously invariant.

where we introduced the gluon fields A_μ^a with $a = 1, \ldots, N_\mathrm{c}^2 - 1$. Furthermore, T^a are the generators of the gauge group $\mathrm{SU}(N_\mathrm{c})$ in the fundamental representation, normalised to $\mathrm{Tr}\big[T^a T^b\big] = \frac{1}{2}\delta_{ab}$, and g_s is the unrenormalised strong coupling constant. Local gauge invariance of $\mathcal{L}_\mathrm{quark}$ is now achieved by demanding a transformation behaviour of the gluon fields such that

$$D'_\mu \psi' = U\,(D_\mu \psi) \tag{2.3}$$

holds. This yields

$$A_\mu^a T^a \to U A_\mu^a T^a U^{-1} + \frac{\mathrm{i}}{g_\mathrm{s}}\,(\partial_\mu U)\,U^{-1}\ . \tag{2.4}$$

After adding the gluons to the theory, we are left with including a dynamic term for them, i.e. a locally invariant term which contains A_μ^a and its derivatives. To this end, we consider the commutator of two covariant derivatives:

$$\begin{aligned} -\frac{\mathrm{i}}{g_\mathrm{s}}\big[D_\mu, D_\nu\big] &= \Big(\partial_\mu A_\nu^a - \partial_\nu A_\mu^a - g_\mathrm{s}\, f^{abc} A_\mu^b A_\nu^c\Big)\, T^a \\ &=: F_{\mu\nu}^a T^a\ , \end{aligned} \tag{2.5}$$

which defines the gluon field strength tensor $F_{\mu\nu}^a$. In Eq. (2.5), f^{abc} are the totally antisymmetric $\mathrm{SU}(N_\mathrm{c})$ structure constants defined by $\big[T^a, T^b\big] = \mathrm{i} f^{abc} T^c$. Using (2.4), the gluon field strength tensor transforms under a gauge transformation according to

$$F_{\mu\nu}^a T^a \to U F_{\mu\nu}^a T^a U^{-1}\ . \tag{2.6}$$

The locally gauge invariant gluon Lagrangian $\mathcal{L}_\mathrm{YM}$ (named after Yang and Mills who first introduced it [36]) is given by

$$\mathcal{L}_\mathrm{YM} := \frac{1}{4} F_{\mu\nu}^a F_{\mu\nu}^a\ . \tag{2.7}$$

Thus, the QCD Lagrangian reads [5, 6]

$$\begin{aligned} \mathcal{L}_\mathrm{QCD} &:= \mathcal{L}_\mathrm{quarks} + \mathcal{L}_\mathrm{YM} \\ &= \bar\psi\,\big(-\not{D} + m\big)\,\psi + \frac{1}{4} F_{\mu\nu}^a F_{\mu\nu}^a\ , \end{aligned} \tag{2.8}$$

which is used to define the generating functional of QCD in the path integral formalism by

$$\mathcal{Z}[J] := \int \mathcal{D}\big[\bar\psi\psi A\big] \exp\!\Big(-I_\mathrm{QCD} + \int \mathrm{d}^4x\,\big(j_\mu^a A_\mu^a + \bar\eta\psi + \bar\psi\eta\big)\Big) \tag{2.9}$$

with the abbreviation $\mathcal{D}\big[\bar\psi\psi A\big] := \mathcal{D}\bar\psi\,\mathcal{D}\psi\,\prod_{\nu,b}\mathcal{D}A_\nu^b$, the sources j_μ^a, $\bar\eta$, η (summarised in the argument J), and the action

$$I_\mathrm{QCD} := \int \mathrm{d}^4x\,\mathcal{L}_\mathrm{QCD}\ . \tag{2.10}$$

2.1.2. Gauge Fixing

The QCD Lagrangian was constructed to be invariant under local gauge transformations

$$\psi \to \psi^{(\vartheta)} := U_\vartheta \psi \ , \qquad \bar{\psi} \to \bar{\psi}^{(\vartheta)} := \bar{\psi} U_\vartheta^{-1} \ , \tag{2.11a}$$

$$A_\mu \to A_\mu^{(\vartheta),a} T^a := U_\vartheta A_\mu^a T^a U_\vartheta^{-1} + \frac{\mathrm{i}}{g_\mathrm{s}} (\partial_\mu U_\vartheta) U_\vartheta^{-1} \ , \tag{2.11b}$$

where $U_\vartheta := \exp\bigl(\mathrm{i}\vartheta^a(x) T^a\bigr) \in \mathrm{SU}(N_\mathrm{c})$ with spacetime-dependent functions $\vartheta^a(x)$ which characterise the transformation. The field configurations generated from a given configuration $\bigl(\psi, \bar{\psi}, A_\mu\bigr)$ by all possible gauge transformations form a set

$$\mathcal{O}\bigl(\psi, \bar{\psi}, A_\mu^a\bigr) := \left\{ \left(\psi^{(\vartheta)}, \bar{\psi}^{(\vartheta)}, A_\mu^{(\vartheta),a} T^a \right) \,:\, U_\vartheta = \exp\bigl(\mathrm{i}\vartheta^a(x) T^a\bigr) \in \mathrm{SU}(N_\mathrm{c}) \right\} , \tag{2.12}$$

the so-called gauge orbit. Since the Lagrangian is invariant under gauge transformations, all configurations contained in a gauge orbit $\mathcal{O}\bigl(\psi, \bar{\psi}, A_\mu^a\bigr)$ yield the same action. Thus, the path integral in (2.9) also covers equivalent configurations, which generates an infinite factor, the volume of the gauge group, which has to be factorised and absorbed into the normalisation of the path integral. Furthermore, the quadratic part $A_\mu^a \bigl(-g_{\mu\nu}\,\partial^2 + \partial_\mu \partial_\nu\bigr) A_\nu^a$ of the gluon Lagrangian has vanishing eigenvalues, preventing the definition of a perturbative gluon propagator.

In order to solve these problems, one has to restrict the path integral to one representative per gauge orbit. The method of gauge fixing proposed by Faddeev and Popov [37] realises this by placing a restriction on the gluon fields, viz. demanding that only field configurations obeying

$$\mathcal{F}[A_\mu^a] = B^a \tag{2.13}$$

are taken into account, where $\mathcal{F}$ is a local functional of A_μ^a. B^a is in principle arbitrary as long as it is independent of the gluon fields and singles out exactly one configuration per gauge orbit. We choose linear covariant gauges, i.e. $\mathcal{F}[A_\mu^a] := \partial_\mu A_\mu^a$, and instead of fixing B^a, one averages over all possible B^a with a Gaussian weight centred on $B^a = 0$. This leads to the gauge-fixed partition function

$$\mathcal{Z}_\mathrm{gf}[J] := \int \left(\prod_b \mathcal{D}B^b \right) \exp\left(-\frac{1}{2\xi} \int \mathrm{d}^4x \, (B^a)^2 \right) \mathcal{Z}[J] \,\Big|_{\mathcal{F}[A_\mu^a] = B^a} \tag{2.14}$$

with a parameter ξ, which determines the width of the Gaussian. The gauge-fixing condition is now implemented by inserting

$$1 = \int \left(\prod_b \mathcal{D}\vartheta^b \right) \prod_{a,x} \delta\Bigl(\mathcal{F}\bigl[A_\mu^{(\vartheta),a}\bigr](x) - B^a(x) \Bigr) \det(\mathcal{M}) \tag{2.15}$$

into the path integrals in (2.14). Here, $\det(\mathcal{M})$ denotes the so-called Faddeev-Popov determinant, where the matrix $\mathcal{M}$ is defined by its elements,

$$\mathcal{M}^{ab} := \frac{\delta \mathcal{F}\bigl[A_\mu^{(\vartheta),a}\bigr]}{\delta \vartheta^b} \ . \tag{2.16}$$

Finally, Faddeev and Popov expressed the determinant as a path integral,

$$\det(\mathcal{M}) = \int \mathcal{D}[\bar{c}c] \exp\left(-\int \mathrm{d}^4x\ \bar{c}^a \mathcal{M}^{ab} c^b\right) , \tag{2.17}$$

to maintain the Lagrangian form of the gauge-fixed generating functional. Consequently, this adds the auxiliary fields c^a and $\bar{c}^a$ to the theory, called ghosts. They have the odd property being anticommuting spin-0 fields. Thus, together with the unphysical gluon polarisations, they have to be absent in the physical spectrum.

Eventually, bringing all pieces together (referring to [34] for a detailed derivation) we arrive at the final form of the gauge-fixed generating functional

$$\mathcal{Z}_{\mathrm{gf}}[J] = \int \mathcal{D}\left[\bar{\psi}\psi A \bar{c}c\right] \exp\left(-I_{\mathrm{gf}} + \int \mathrm{d}^4x \left(j_\mu^a A_\mu^a + \bar{\eta}\psi + \bar{\psi}\eta + \bar{\sigma}^a c^a + \bar{c}^a \sigma^a\right)\right) \tag{2.18}$$

with additional sources $\bar{\sigma}^a$, σ^a for the ghost fields and the action

$$I_{\mathrm{gf}} := \int \mathrm{d}^4x\ \mathcal{L}_{\mathrm{gf}} \tag{2.19}$$

with the gauge-fixed QCD Lagrangian

$$\mathcal{L}_{\mathrm{gf}} := \mathcal{L}_{\mathrm{QCD}} + \frac{1}{2\xi}\left(\partial_\mu A_\mu^a\right)^2 + \bar{c}^a \left(\partial_\mu D_\mu^{ab}\right) c^b , \tag{2.20}$$

where $D_\mu^{ab} = \delta_{ab}\partial_\mu + g_\mathrm{s} f^{abc} A_\mu^c$ denotes the covariant derivative in the adjoint representation of the gauge group. Furthermore, the gauge parameter ξ can be chosen freely. In this work, we use Landau gauge, defined by $\xi \to 0$. Thus, the gauge condition reads $\partial_\mu A_\mu^a = 0$, i.e. the gluons are purely transverse.

Finally, we would like to add two remarks:

- The gauge-fixing procedure summarised above breaks of course local gauge invariance. However, $\mathcal{L}_{\mathrm{gf}}$ is still invariant under a transformation discovered by Becchi, Rouet, and Stora [38–40] and independently by Tyutin [41, 42]. This so-called BRST transformation ensures the absence of ghosts and unphysical gluon polarisations in the physical spectrum. A detailed discussion can be found in Refs. [34, 43].
- Eq. (2.15) is accompanied by the tacit assumptions that the argument of the delta function has only one zero and that the Faddeev-Popov determinant is positive. In general, both assumptions are not true. It can be shown that the Faddeev-Popov determinant is only positive in the vicinity of $A_\mu^a = 0$ (i.e. in perturbation theory). Furthermore, there exists distinct gluon fields fulfilling the Landau gauge condition that are related by a gauge transformation [44]. Even worse, for a non-Abelian gauge group there exists no local function B^a (cf. Eq. (2.13)) which singles out exactly one field configuration per gauge

orbit [45]. A solution of this problem is by no means simple and a first approach is to restrict the path integral to the region where the Faddeev-Popov determinant is positive. Unfortunately, this does not solve the problem completely. A detailed discussion can be found in Ref. [46]. However, we assume that the path integral (2.18) is well defined.

2.1.3. Generating Functionals and Correlation Functions

Before we proceed, we shall generalise the above to several quark flavours: We now treat the quark field ψ as an N_f-component vector in flavour space where each component is an N_c-component vector in colour space with components being Dirac spinors. Furthermore, for the sake of brevity, we collect the fields and corresponding sources in tuples $\phi := \left(\overline{\psi}_\alpha, \psi_\alpha, A^a_\mu, \overline{c}^a, c^a\right)$ and $J := \left(\eta_\alpha, \overline{\eta}_\alpha, j^a_\mu, \sigma^a, \overline{\sigma}^a\right)$. Here, α denotes a collective index, summarising flavour, colour, and Dirac degrees of freedom.

Now, having the gauge-fixed generating functional at hand, we can derive correlation functions (in presence of the sources) by taking functional derivatives of $\mathcal{Z}_\mathrm{gf}$ with respect to the sources. Generically,

$$\langle \phi_i(x_1)\phi_j(x_2)\ldots\rangle_J := \pm\frac{1}{\mathcal{Z}_\mathrm{gf}[J]}\frac{\delta^n \mathcal{Z}_\mathrm{gf}[J]}{\delta J_i(x_1)\delta J_j(x_2)\ldots} \,. \tag{2.21}$$

Note that the physical correlation functions are obtained by setting $J = 0$. However, correlation functions generated in this way contain disconnected and connected parts. Usually, one is only interested in the latter and it is advantageous to define

$$W[J] := \log(\mathcal{Z}_\mathrm{gf}[J]) \,, \tag{2.22}$$

which generates only connected correlation functions. The simplest case are the one-point correlation functions, i.e. the expectation values of the fields in presence of the sources, called the macroscopic fields Φ_i:

$$\frac{\delta W[J]}{\delta J_i(x)} = \pm\langle\phi_i(x)\rangle_J =: \pm\Phi_i(x) \tag{2.23}$$

where the plus sign stands for $J_i \in \left\{j^a_\mu, \overline{\eta}_\alpha, \overline{\sigma}^a\right\}$ and the minus sign for $J_i \in \left\{\eta_\alpha, \sigma^a\right\}$, where the latter emerges from exchanging Graßmann-valued quantities [3]. Explicitly, the macroscopic fields of the quarks, gluons, and ghosts are denoted by $\overline{\Psi}_\alpha$, Ψ_α, $\mathcal{A}^a_\mu$, $\overline{\mathcal{C}}^a$, and $\mathcal{C}^a$, respectively. A Legendre transform of $W[J]$ yields the one-particle irreducible (1PI) effective action [47]

$$\Gamma_\mathrm{1PI}[\Phi] := \int \mathrm{d}^4x \left(\overline{\Psi}_\alpha\eta_\alpha + \overline{\eta}_\alpha\Psi_\alpha + j^a_\mu\mathcal{A}^a_\mu + \overline{\mathcal{C}}^a\sigma^a + \overline{\sigma}^a\mathcal{C}^a\right) - W[J] \,. \tag{2.24}$$

This implies that the sources are given by

$$\frac{\delta\Gamma_\mathrm{1PI}[\Phi]}{\delta\Phi_i(x)} = \pm J_i(x) \,, \tag{2.25}$$

[3] All functional derivatives act from the left like ordinary derivatives.

where the upper sign applies to $\Phi_i \in \{\mathcal{A}^a_\mu, \bar{\Psi}_\alpha, \bar{\mathcal{C}}^a\}$ and the lower sign to $\Phi_i \in \{\Psi_\alpha, \mathcal{C}^a\}$. Furthermore, the physical dressed quark, gluon, and ghost propagators $S_{\alpha\beta}$, $D^{ab}_{\mu\nu}$, and G^{ab} are defined as two-point functions with vanishing sources and can be expressed either by derivatives of $W[J]$ or $\Gamma_{\mathrm{1PI}}[\Phi]$:

$$S_{\alpha\beta}(x,y) := \left.\frac{\delta^2 W[J]}{\delta\eta_\beta(y)\,\delta\bar{\eta}_\alpha(x)}\right|_{J=0} = \left(\frac{\delta^2\Gamma_{\mathrm{1PI}}[\Phi]}{\delta\Psi_\beta(y)\,\delta\bar{\Psi}_\alpha(x)}\right)^{-1}, \tag{2.26a}$$

$$D^{ab}_{\mu\nu}(x,y) := \left.\frac{\delta^2 W[J]}{\delta j^b_\nu(y)\,\delta j^a_\mu(x)}\right|_{J=0} = \left(\frac{\delta^2\Gamma_{\mathrm{1PI}}[\Phi]}{\delta\mathcal{A}^b_\nu(y)\,\delta\mathcal{A}^a_\mu(x)}\right)^{-1}, \tag{2.26b}$$

$$G^{ab}(x,y) := \left.\frac{\delta^2 W[J]}{\delta\sigma^b(y)\,\delta\bar{\sigma}^a(x)}\right|_{J=0} = \left(\frac{\delta^2\Gamma_{\mathrm{1PI}}[\Phi]}{\delta\mathcal{C}^b(y)\,\delta\bar{\mathcal{C}}^a(x)}\right)^{-1}, \tag{2.26c}$$

where the right hand side has to be evaluated at the stationary point, i.e. at the value of Φ for which $\delta\Gamma_{\mathrm{1PI}}/\delta\Phi = 0$. The bare propagators are obtained from $\Gamma_{\mathrm{1PI}}[\Phi] = I_{\mathrm{gf}}[\Phi]$ for vanishing macroscopic fields, e.g.

$$S^{-1}_{0,\alpha\beta}(x,y) := \left.\frac{\delta^2 I_{\mathrm{gf}}[\Phi]}{\delta\Psi_\beta(y)\,\delta\bar{\Psi}_\alpha(x)}\right|_{\Phi=0} = \left(-\not{\partial} + m\right)_{\alpha\beta}\delta^{(4)}(x-y) \tag{2.27}$$

is the bare quark propagator.

The dressed vertices are n-point functions with $n > 2$. For example, the dressed quark-gluon vertex $\Gamma^a_{\mu,\alpha\beta}$ is defined by

$$g_{\mathrm{s}}\,\Gamma^a_{\mu,\alpha\beta}(x,y,z) := \frac{\delta^3\Gamma_{\mathrm{1PI}}[\Phi]}{\delta\mathcal{A}^a_\mu(x)\,\delta\Psi_\beta(z)\,\delta\bar{\Psi}_\alpha(y)}\,. \tag{2.28}$$

For its Fourier transform, we define the gluon momentum k to be incoming whereas the quark momenta q and p are defined such that the former is incoming and the latter outgoing (cf. Figure 2.1), i.e.

$$g_{\mathrm{s}}\,\Gamma^a_{\mu,\alpha\beta}(k,q,p) = \iiint \mathrm{d}^4x\,\mathrm{d}^4y\,\mathrm{d}^4z\; g_{\mathrm{s}}\,\Gamma^a_{\mu,\alpha\beta}(x,y,z)\,\mathrm{e}^{-\mathrm{i}k\cdot x}\,\mathrm{e}^{-\mathrm{i}q\cdot x}\,\mathrm{e}^{\mathrm{i}p\cdot x}\,. \tag{2.29}$$

Furthermore, momentum conservation allows to define a reduced vertex via

$$g_{\mathrm{s}}\,\Gamma^a_{\mu,\alpha\beta}(k,q,p) = -\mathrm{i}\,g_{\mathrm{s}}(2\pi)^4\,\delta^{(4)}(k+q-p)\,\Gamma^a_{\mu,\alpha\beta}(q,p)\,, \tag{2.30}$$

which entails $k = p - q$ for the gluon momentum.

2.1.4. Renormalisation

In specific calculations, one encounters divergent integrals which have to be regularised. This introduces a regularisation parameter Λ (e.g. a sharp momentum cutoff). Consequently, quantities like correlation functions calculated from these regularised integrals depend on this artifical

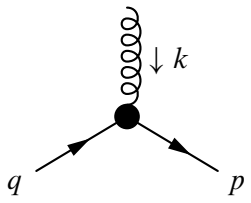

Figure 2.1.: Momentum flow for the dressed quark-gluon vertex (depicted as a thick dot). The quarks are depicted as straight lines and the gluons is represented by a curly line.

parameter. Fortunately, the gauge-fixed Lagrangian given in (2.19) is multiplicatively renormalisable [48, 49]. Thus, the introduction of a finite number of renormalisation constants Z_i removes all occuring divergencies and the results are finite and independent of Λ. Instead, renormalised quantities depend on a renormalisation scale ζ, at which the physical parameters of the theory are defined. The transition from regularisation parameter dependence to renormalisation point dependence is encoded in the renormalisation constants, thus they are functions of ζ and Λ.

To obtain a renormalised theory, the fields, the coupling constant, and the mass are rescaled according to

$$\begin{aligned} \bar{\psi}\psi \;\to\; Z_2\,\bar{\psi}\psi\;, \qquad A^a_\mu \;\to\; \sqrt{Z_3}\,A^a_\mu\;, \qquad \bar{c}^a c^b \;\to\; \widetilde{Z}_3\,\bar{c}^a c^b \\ g_\mathrm{s} \;\to\; Z_{g_\mathrm{s}}\,g_\mathrm{s}\;, \qquad m \;\to\; Z_m m\;, \end{aligned} \tag{2.31}$$

where Z_2, Z_3, $\widetilde{Z}_3$, Z_{g_s}, and Z_m are the quark, gluon, ghost, coupling constant, and mass renormalisation constant, respectively. The renormalised, gauge-fixed QCD Lagrangian is explicitly given by

$$\begin{aligned} \mathscr{L}_{\mathrm{gf,R}} := {} & Z_2\,\bar{\psi}\left(-\not{\partial} + Z_m m\right)\psi - Z_{1\mathrm{F}}\,\mathrm{i}\,g_\mathrm{s}\,\bar{\psi}\not{A}^a T^a\,\psi + \frac{Z_3}{4}\left(\partial_\mu A^a_\nu - \partial_\nu A^a_\mu\right)^2 \\ & - Z_1\,g_\mathrm{s}\,f^{abc}\left(\partial_\mu A^a_\nu\right)A^b_\mu A^c_\nu + \frac{Z_4}{4}\,g_\mathrm{s}^2\,f^{abe}\,f^{cde}\,A^a_\mu A^b_\nu A^c_\mu A^d_\nu \\ & + \widetilde{Z}_3\,\bar{c}^a\partial^2 c^a + \widetilde{Z}_1\,g_\mathrm{s}\,f^{abc}\,\bar{c}^a\partial_\mu\left(c^b A^c_\mu\right) + \frac{1}{2\xi}\left(\partial_\mu A^a_\mu\right)^2 \end{aligned} \tag{2.32}$$

with additional renormalisation constants $Z_{1\mathrm{F}}$, Z_1, Z_4, and $\widetilde{Z}_1$ for the quark-gluon, three-gluon, four-gluon, and ghost-gluon vertex, respectively. These renormalisation constants are not independent but related to the those in (2.31) via

$$\begin{aligned} Z_{1\mathrm{F}} &= Z_{g_\mathrm{s}} Z_2 \sqrt{Z_3}\;, \qquad Z_1 = Z_{g_\mathrm{s}} Z_3^{3/2}\;, \\ Z_4 &= \left(Z_{g_\mathrm{s}} Z_3\right)^2\;, \qquad \widetilde{Z}_1 = Z_{g_\mathrm{s}}\widetilde{Z}_3\sqrt{Z_3}\;. \end{aligned} \tag{2.33}$$

These relations are called Slavnov–Taylor identities [50, 51] and obtained by exploiting the BRST invariance of the Lagrangian. Note that it is not necessary to introduce a renormalisation

constant for the last term in (2.32), since its only purpose is to implement the Landau gauge condition $\partial_\mu A^a_\mu = 0$ and is therefore insensitive to a rescaling of the gluon field. Furthermore, Landau gauge entails $\widetilde{Z}_1 = 1$ [51], yielding

$$Z_{g_\mathrm{s}} = \frac{1}{\widetilde{Z}_3 \sqrt{Z_3}} , \qquad Z_{1\mathrm{F}} = \frac{Z_2}{\widetilde{Z}_3} . \tag{2.34}$$

Consequently, the correlation functions introduced in Section 2.1.3 inherit the renormalisation dependence. The unrenormalised quark, gluon, and ghost propagators (indicated by an additional dependence on Λ) are related to their renormalised versions (indicated by an additional dependence on ζ) by

$$S_{\alpha\beta}(x, y; \Lambda) = Z_2 \, S_{\alpha\beta}(x, y; \zeta) , \tag{2.35a}$$

$$D^{ab}_{\mu\nu}(x, y; \Lambda) = Z_3 \, D^{ab}_{\mu\nu}(x, y; \zeta) , \tag{2.35b}$$

$$G^{ab}(x, y; \Lambda) = \widetilde{Z}_3 \, G^{ab}(x, y; \zeta) . \tag{2.35c}$$

Finally, the gauge-fixed and renormalised action is defined by

$$I_{\mathrm{gf,R}} := \int \mathrm{d}^4 x \, \mathscr{L}_{\mathrm{gf,R}} . \tag{2.36}$$

2.1.5. QCD at Nonzero Temperature and Density

Since our goal is the calculation of Taylor coefficients of the quark pressure, we have to consider QCD at nonzero temperature and density. To this end, the system is coupled to a heat bath, i.e. the system is described with respect to the heat bath's reference frame which leads to a preferred direction, given by the four-velocity u_μ of the heat bath. Without loss of generality, we use $u_\mu = (1, 0, 0, 0)$ (i.e. the reference frame mentioned before is the rest frame of the medium). Consequently, the original O(4) symmetry is broken to O(3), since the symmetry of the coordinates perpendicular to u_μ, which are precisely the spatial coordinates, remains.

Nonzero temperature $T > 0$ is introduced by restricting the (Euclidean) time integration to the interval $[0, 1/T]$, i.e.

$$\int \mathrm{d}^4 x \, f(x) \;\to\; \int_0^{1/T} \mathrm{d}x_4 \int \mathrm{d}^3 \boldsymbol{x} \, f\big(x = (x_4, \boldsymbol{x})\big) , \tag{2.37}$$

In momentum space, this replaces the integral over the (Euclidean) energy component p_4 of the momentum with a sum over discrete frequencies ω_n,

$$\int \frac{\mathrm{d}^4 p}{(2\pi)^4} \, f(p) \;\to\; T \sum_{n=-\infty}^{\infty} \int \frac{\mathrm{d}^3 \boldsymbol{p}}{(2\pi)^3} \, f\big(p = (\omega_n, \boldsymbol{p})\big) , \tag{2.38}$$

called Matsubara frequencies [52]. These differ for fermions and bosons, since the former obey antiperiodic boundary conditions, e.g. $\psi(0,\boldsymbol{x}) = -\psi(1/T,\boldsymbol{x})$ for quarks, and the latter periodic boundary conditions, e.g. $A^a_\mu(0,\boldsymbol{x}) = A^a_\mu(1/T,\boldsymbol{x})$ for gluons. Thus, the Matsubara frequencies are given by

$$\omega_n := \begin{cases} (2n+1)\pi T & \text{for fermions}\,, \\ 2n\pi T & \text{for bosons}\,. \end{cases} \tag{2.39}$$

Finally, nonzero quark chemical potential $\mu > 0$ is introduced as a Lagrange multiplier in the action

$$I_{\mathrm{gf}} = \int_0^{1/T} \mathrm{d}x_4 \int \mathrm{d}^3\boldsymbol{x}\, \left(\mathscr{L}_{\mathrm{gf}} + \mu\,\psi^\dagger\psi\right), \tag{2.40}$$

enforcing baryon number conservation. Since $\psi^\dagger\psi = \overline{\psi}\gamma_4\psi$, the dependence on the chemical potential can be included in the quark Lagrangian

$$\mathscr{L}_{\mathrm{quark}} \;\to\; \mathscr{L}_{\mathrm{quark}} + \mu\,\psi^\dagger\psi = \overline{\psi}\left(-\not{D} + m + \mu\,\gamma_4\right)\psi\,. \tag{2.41}$$

2.2. Dyson–Schwinger Equations

The Dyson–Schwinger equations (DSEs) are coupled integral equations for the correlation functions of a theory and obtained from the action of the theory without any approximation and are therefore exact. They were first discovered by Dyson and Schwinger [17–19], for a comprehensive review we refer to Refs. [53–57].

The starting point for the derivation of the DSEs in vacuum is the identity (see App. B)

$$0 = \int \mathscr{D}\phi\, \frac{\delta}{\delta\phi_i(x)} \exp\!\left(-I_{\mathrm{gf,R}}[\phi] + \int \mathrm{d}^4y\, \left(j^a_\mu A^a_\mu + \overline{\eta}_\alpha\psi_\alpha + \overline{\psi}_\alpha\eta_\alpha + \overline{\sigma}^a c^a + \overline{c}^a\sigma^a\right)\right). \tag{2.42}$$

Carrying out the derivative, we can write

$$\begin{aligned} 0 &= \int \mathscr{D}\phi \left(-\frac{\delta I_{\mathrm{gf,R}}[\phi]}{\delta\phi_i(x)} \pm J_i(x)\right) \\ &\quad\times \exp\!\left(-I_{\mathrm{gf,R}}[\phi] + \int \mathrm{d}^4x\, \left(j^a_\mu A^a_\mu + \overline{\eta}_\alpha\psi_\alpha + \overline{\psi}_\alpha\eta_\alpha + \overline{\sigma}^a c^a + \overline{c}^a\sigma^a\right)\right) \\ &= \left(-\frac{\delta I_{\mathrm{gf,R}}[\phi]}{\delta\phi_i(x)}\left[\phi_j \to \pm\frac{\delta}{\delta J_j}\right] + \frac{\delta\Gamma_{1\mathrm{PI}}[\Phi]}{\delta\Phi_i(x)}\right)\mathscr{Z}_{\mathrm{gf,R}}[J] \\ &= \left(-\frac{\delta I_{\mathrm{gf,R}}[\phi]}{\delta\phi_i(x)}\left[\phi_j \to \pm\frac{\delta}{\delta J_j}\right] + \frac{\delta\Gamma_{1\mathrm{PI}}[\Phi]}{\delta\Phi_i(x)}\right)\exp(W[J]) \end{aligned} \tag{2.43}$$

where we used Eq. (2.25) to replace the sources with derivatives of the 1PI effective action. Concerning the substitution of the fields with derivatives, the plus sign applies to $\phi_j \in \left\{A^a_\mu, \psi_\alpha, c^a\right\}$ and the minus sign to $\phi_j \in \left\{\bar{\psi}_\alpha, \bar{c}^a\right\}$. Eq. (2.43) can be rewritten even further to obtain

$$\frac{\delta \Gamma_{1\mathrm{PI}}[\Phi]}{\delta \Phi_i(x)} = \frac{\delta I_{\mathrm{gf,R}}[\phi]}{\delta \phi_i(x)}\left[\phi_j \to \pm\left(\frac{\delta}{\delta J_j} + \frac{\delta W[J]}{\delta J_j}\right)\right] 1 \,, \tag{2.44}$$

which is regarded as the generating DSE for all n-point correlation functions. From this equation, all DSEs can be derived in the following way:

- Evaluate (2.44) with appropriate fields ϕ_i, Φ_i and replace the quantities $\delta W/\delta J_j$ with the corresponding classical fields Φ_j.
- Perform $n-1$ further derivatives with respect to appropriate fields Φ_j on the left and right hand side of the result obtained from the previous step.
- Set $J = 0$ to obtain the DSE for the physical n-point correlation function.

Derivation of the Dyson–Schwinger Equation for the Quark Propagator

Since the DSE for the quark propagator (qDSE) plays an important part in this work, we shall derive it in the following using the recipe described above. The qDSE is obtained by choosing $\phi_i = \bar{\psi}_\alpha$ and $\Phi_i = \bar{\Psi}_\alpha$, respectively. The derivative of the action reads

$$\frac{\delta I_{\mathrm{gf,R}}[\phi]}{\delta \bar{\psi}_\alpha(x)} = \left[Z_2\left(-\not{\partial} + Z_m m\right) - Z_{1\mathrm{F}}\,\mathrm{i}\,g_\mathrm{s}\,\not{A}^a T^a\right]_{\alpha\delta}\psi_\delta(x) \tag{2.45}$$

and the right hand side of Eq. (2.44) is then given by

$$\begin{aligned}
&\frac{\delta I_{\mathrm{gf,R}}[\phi]}{\delta \bar{\psi}_\alpha(x)}\left[\psi_\delta \to \frac{\delta W[J]}{\delta \bar{\eta}_\delta} + \frac{\delta}{\delta \bar{\eta}_\delta}\,,\ A^a_\mu \to \frac{\delta W[J]}{\delta j^a_\mu} + \frac{\delta}{\delta j^a_\mu}\right] 1 \\
&= \left[Z_2\left(-\not{\partial} + Z_m m\right) - Z_{1\mathrm{F}}\,\mathrm{i}\,g_\mathrm{s}\,\gamma_\mu\left(\frac{\delta W[J]}{\delta j^a_\mu(x)} + \frac{\delta}{\delta j^a_\mu(x)}\right)T^a\right]_{\alpha\delta}\left(\frac{\delta W[J]}{\delta \bar{\eta}_\delta(x)} + \frac{\delta}{\delta \bar{\eta}_\delta(x)}\right) 1 \\
&= Z_2\left(-\not{\partial} + Z_m m\right)_{\alpha\delta}\Psi_\delta(x) - Z_{1\mathrm{F}}\,\mathrm{i}\,g_\mathrm{s}\left(\gamma_\mu T^a\right)_{\alpha\delta}\left(\frac{\delta \Psi_\delta(x)}{\delta j^a_\mu(x)} + \mathcal{A}^a_\mu(x)\,\Psi_\delta(x)\right) .
\end{aligned} \tag{2.46}$$

For the moment, the left hand side of Eq. (2.44) reads $\delta\Gamma_{1\mathrm{PI}}[\Phi]/\delta\bar{\Psi}_\alpha(x)$. A subsequent derivative with respect to $\Psi_\beta(y)$ yields the inverse dressed quark propagator (cf. Eq. (2.26a)). Thus, we find

$$\begin{aligned}
S^{-1}_{\alpha\beta}(x,y) = {}& Z_2\left(-\not{\partial} + Z_m m\right)_{\alpha\beta}\delta^{(4)}(x-y) \\
&- Z_{1\mathrm{F}}\,\mathrm{i}\,g_\mathrm{s}\left(\gamma_\mu T^a\right)_{\alpha\delta}\left(\frac{\delta^2 \Psi_\delta(x)}{\delta\Psi_\beta(y)\,\delta j^a_\mu(x)} + \frac{\delta}{\delta\Psi_\beta(y)}\left(\mathcal{A}^a_\mu(x)\,\Psi_\delta(x)\right)\right) .
\end{aligned} \tag{2.47}$$

Using the functional chain rule and Eq. (2.25) yields

$$S^{-1}_{\alpha\beta}(x,y) = Z_2\left(-\not{\partial} + Z_m m\right)_{\alpha\beta}\delta^{(4)}(x-y) - Z_{1\mathrm{F}}\mathrm{i}g_\mathrm{s}\left(\gamma_\mu T^a\right)_{\alpha\delta}\int \mathrm{d}^4 z\,(\pm)\frac{\delta^2\Gamma_{1\mathrm{PI}}[\Phi]}{\delta\Psi_\beta(y)\delta\Phi_i(z)}\left(\frac{\delta^3 W[J]}{\delta J_i(z)\delta j^a_\mu(x)\delta\overline{\eta}_\delta(x)} + \frac{\delta}{\delta J_i(z)}\left(\mathcal{A}^a_\mu(x)\Psi_\delta(x)\right)\right) \tag{2.48}$$

Now, we set the sources to zero to obtain the physical correlation functions. In this case, the only nonvanishing contribution from the chain rule is $\Phi_i = \bar{\Psi}$. Thus, using (2.26a),

$$S^{-1}_{\alpha\beta}(x,y) = Z_2\left(-\not{\partial} + Z_m m\right)_{\alpha\beta}\delta^{(4)}(x-y) - Z_{1\mathrm{F}}\mathrm{i}g_\mathrm{s}\left(\gamma_\mu T^a\right)_{\alpha\delta}\int \mathrm{d}^4 z\,\frac{\delta^2\Gamma_{1\mathrm{PI}}[\Phi]}{\delta\Psi_\beta(y)\delta\bar{\Psi}_\varepsilon(z)}\frac{\delta}{\delta j^a_\mu(x)}\left(\frac{\delta^2\Gamma_{1\mathrm{PI}}[\Phi]}{\delta\Psi_\varepsilon(z)\delta\bar{\Psi}_\delta(x)}\right)^{-1}. \tag{2.49}$$

The derivative of the inverse second derivative of the effective action is evaluated using the identity $\delta M^{-1} = -M^{-1}(\delta M)M^{-1}$, which is reminiscent of finite-dimensional matrix calculus. Finally, we arrive at

$$S^{-1}_{\alpha\beta}(x,y) = Z_2\left(-\not{\partial} + Z_m m\right)_{\alpha\beta}\delta^{(4)}(x-y) + Z_{1\mathrm{F}}\mathrm{i}g_\mathrm{s}\left(\gamma_\mu T^a\right)_{\alpha\delta} \times \iint \mathrm{d}^4 z\,\mathrm{d}^4 z'\,\frac{\delta^2 W[J]}{\delta j^a_\mu(x)\delta j^b_\nu(z)}\frac{\delta^3\Gamma_{1\mathrm{PI}}[\Phi]}{\delta\mathcal{A}^b_\nu(z)\delta\Psi_\beta(y)\delta\bar{\Psi}_\varepsilon(z')}\frac{\delta^2 W[J]}{\delta\Psi_\varepsilon(z')\delta\bar{\Psi}_\delta(x)}. \tag{2.50}$$

Now we have to make some identifications to put the result in a more common form. Since the bare propagators are defined as the corresponding derivatives of the action evaluated at vanishing macroscopic fields, the first term in (2.50) is readily identified as the inverse bare quark propagator

$$S^{-1}_{0,\alpha\beta}(x,y) = Z_2\left(-\not{\partial} + Z_m m\right)_{\alpha\beta}\delta^{(4)}(x-y)\,. \tag{2.51}$$

The second term corresponds to the quark self-energy, which is defined as

$$\Sigma_{\alpha\beta}(x,y) := Z_{1\mathrm{F}}\mathrm{i}g_\mathrm{s}\left(\gamma_\mu T^a\right)_{\alpha\delta} \times \iint \mathrm{d}^4 z\,\mathrm{d}^4 z'\,\frac{\delta^2 W[J]}{\delta j^a_\mu(x)\delta j^b_\nu(z)}\frac{\delta^3\Gamma_{1\mathrm{PI}}[\Phi]}{\delta\mathcal{A}^b_\nu(z)\delta\Psi_\beta(y)\delta\bar{\Psi}_\varepsilon(z')}\frac{\delta^2 W[J]}{\delta\Psi_\varepsilon(z')\delta\bar{\Psi}_\delta(x)}. \tag{2.52}$$

Eventually, using (2.26a), (2.26b) and the definition (2.28) of the dressed quark-gluon vertex, we arrive at the qDSE in coordinate space

$$S^{-1}_{\alpha\beta}(x,y) = S^{-1}_{0,\alpha\beta}(x,y) + \Sigma_{\alpha\beta}(x,y) \tag{2.53}$$

with the self-energy

$$\Sigma_{\alpha\beta}(x,y) = Z_{1\mathrm{F}}\,\mathrm{i}\,g_\mathrm{s}^2\left(\gamma_\mu T^a\right)_{\alpha\delta} \iint \mathrm{d}^4z\,\mathrm{d}^4z'\, D^{ab}_{\mu\nu}(x,z)\,S_{\delta\varepsilon}(x,z')\,\Gamma^b_{\nu,\varepsilon\beta}(z,z',y)\;. \tag{2.54}$$

Up to this point, we have the qDSE at hand in coordinate space only. Since the momentum space is in general more advantageous, we Fourier transform Eq. (2.53) with the assumption of a homogenous system, i.e. the propagators and the self-energy depend only on the relative distance $x - y$ and therefore on one single momentum after the Fourier transform. Furthermore, we exploit momentum conservation at the quark-gluon vertex and use Eq. (2.30). Thus, the qDSE in momentum space is given by

$$S^{-1}_{\alpha\beta}(p) = S^{-1}_{0,\alpha\beta}(p) + \Sigma_{\alpha\beta}(p) \tag{2.55}$$

with the inverse bare quark propagator

$$S^{-1}_{0,\alpha\beta}(p) = Z_2\left(-\mathrm{i}\not{p} + Z_m\,m\right)_{\alpha\beta} \tag{2.56}$$

and the self-energy

$$\Sigma_{\alpha\beta}(p) = Z_{1\mathrm{F}}\,g_\mathrm{s}^2\left(\gamma_\mu T^a\right)_{\alpha\delta} \int \frac{\mathrm{d}^4q}{(2\pi)^4}\, D^{ab}_{\mu\nu}(k)\,S_{\delta\varepsilon}(q)\,\Gamma^b_{\nu,\varepsilon\beta}(q,p)\;, \tag{2.57}$$

where $k := p - q$ defines the momentum flow.

The qDSE can also be represented diagrammatically, namely

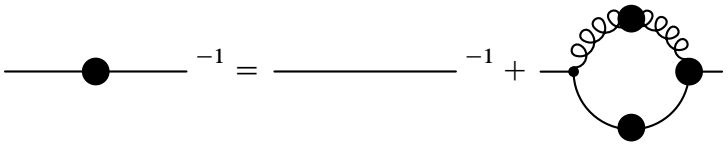

(2.58)

where plain lines representing quark propagators, curly lines gluon propagators, and circles on the joints vertices. Dressed quantities are indicated by a thick dot and the small dot in the self-energy loop diagram is the bare quark-gluon vertex $Z_{1\mathrm{F}}\,g_\mathrm{s}\,\gamma_\mu T^a$.

Nonzero Temperature and Density

The description of QCD at nonzero temperature T and quark chemical potential μ is summarised in Section 2.1.5. Having this in mind, the most important difference to the vacuum is that the propagators depend now separately on a Matsubara frequency and the spatial three-momentum.

The same applies to the dressed quark-gluon vertex, which depends separately on two Matsubara frequencies and two three-momenta. Furthermore, the chemical potential enters as an external parameter. Thus, the qDSE at nonzero T and μ reads

$$S^{-1}_{\alpha\beta}(\omega_n, \boldsymbol{p}; \mu) = S^{-1}_{0,\alpha\beta}(\omega_n, \boldsymbol{p}; \mu) + \Sigma_{\alpha\beta}(\omega_n, \boldsymbol{p}; \mu) \,, \tag{2.59}$$

with the inverse bare quark propagator

$$S^{-1}_{0,\alpha\beta}(\omega_n, \boldsymbol{p}; \mu) = Z_2 \left(-\mathrm{i}\widetilde{\omega}_n \gamma_4 - \mathrm{i}\not{\boldsymbol{p}} + Z_m m\right)_{\alpha\beta} \tag{2.60}$$

and the self-energy

$$\begin{aligned} \Sigma_{\alpha\beta}(\omega_n, \boldsymbol{p}; \mu) = {} & Z_{1\mathrm{F}} g_\mathrm{s}^2 \left(\gamma_\nu T^a\right)_{\alpha\delta} \\ & \times T \sum_{l=-\infty}^{\infty} \int \frac{\mathrm{d}^3\boldsymbol{q}}{(2\pi)^3} \, D^{ab}_{\nu\rho}(\Omega_{nl}, \boldsymbol{k}) \, S_{\delta\varepsilon}(\omega_l, \boldsymbol{q}; \mu) \, \Gamma^b_{\rho,\varepsilon\beta}(\omega_l, \boldsymbol{q}, \omega_n, \boldsymbol{p}; \mu) \,. \end{aligned} \tag{2.61}$$

In the above equations, the yet unknown quantities are given by $\widetilde{\omega}_n := \omega_n + \mathrm{i}\mu$, $\boldsymbol{k} := \boldsymbol{p} - \boldsymbol{q}$, and $\Omega_{nl} := \omega_n - \omega_l$.

3. Solving the Quark Dyson–Schwinger Equation

In the last chapter we derived the DSE for the renormalised quark propagator (qDSE). Recalling its diagrammatic form

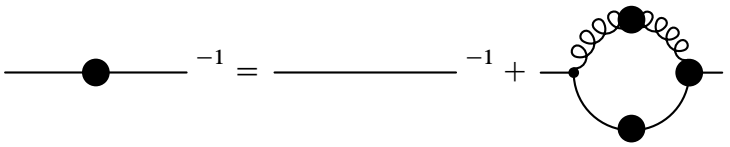

(3.1)

one recognises that the dressed quark propagator, the quantity we want to solve for, appears on both sides of the equation. Thus, the qDSE has to be solved self-consistently. Unfortunately, the equation contains two unknown quantities: The dressed gluon propagator, which reads in vacuum

$$D^{ab}_{\mu\nu}(k) = \delta_{ab}\left(\delta_{\mu\nu} - \frac{k_\mu k_\nu}{k^2}\right)\frac{Z_{\mathrm{YM}}(k^2)}{k^2} \tag{3.2}$$

with the gluon dressing $Z_{\mathrm{YM}}(k^2)$, and the dressed quark-gluon vertex. The dependence on the latter is a feature shared by other DSEs as well, namely that a DSE for an n-point correlation function depends on an $(n+1)$-point correlation function, which obeys again its own DSE. Thus, one has to solve an infinite number of coupled equations. This is sometimes referred to as the "infinite tower of DSEs". As a consequence, truncations are necessary to obtain a finite system of equations, which are solved numerically.

3.1. Vacuum Solutions

3.1.1. Truncation of the Quark Dyson–Schwinger Equation

The qDSE (2.55) has still a rather complicated form for a numerical treatment. It contains a multi-layered index-structure (summarising flavour, colour, and Dirac degrees of freedom) and depends as above-mentioned on the dressed gluon propagator and the dressed quark-gluon vertex. The first step is to reduce the index structure of the equation. One important observation is that the only flavour dependence originates from the quark mass [1]. Thus, the qDSE for a generic flavour f reads

$$S^{-1}_{\alpha\beta}(p) = Z_2\left(-\mathrm{i}\not{p} + Z_m m_f\right)_{\alpha\beta} + Z_{1\mathrm{F}} g_s^2 \left(\gamma_\mu T^a\right)_{\alpha\delta} \int \frac{\mathrm{d}^4 q}{(2\pi)^4}\, D^{ab}_{\mu\nu}(k)\, S_{\delta\varepsilon}(q)\, \Gamma^b_{\nu,\varepsilon\beta}(q,p)\ , \tag{3.3}$$

[1] We assume that all renormalisation constants are flavour-independent.

where the collective indices α, β, etc. now summarising colour and Dirac degrees of freedom only. As defined in the previous chapter, the gluon momentum is always given by $k = p - q$. To simplify the index structure even further, we do not resolve the Dirac structure explicitly for the sake of brevity, use the fact that the propagators are diagonal in colour space, and assume that the colour dependence of the quark-gluon vertex factorises, i.e.

$$S^{-1}_{\alpha\beta} = \delta_{\alpha\beta}\, S^{-1} \,, \qquad D^{ab}_{\mu\nu} = \delta_{ab}\, D_{\mu\nu} \,, \qquad \Gamma^{b}_{\nu,\varepsilon\beta} = \left(T^b\right)_{\varepsilon\beta} \Gamma_\nu \,, \tag{3.4}$$

where the indices α, β, and ε are now colour degrees of freedom only. Finally, after inserting this factorisations into (3.3) and taking the colour trace we arrive at

$$S^{-1}(p) = Z_2\left(-\mathrm{i}\not{p} + Z_m m_f\right) + \frac{4}{3} Z_{1\mathrm{F}} g_\mathrm{s}^2 \int \frac{\mathrm{d}^4 q}{(2\pi)^4}\, \gamma_\mu D_{\mu\nu}(k)\, S(q)\, \Gamma_\nu(q,p) \,. \tag{3.5}$$

At this point, we reduced the index structure of the qDSE to Dirac degrees of freedom only. However, we are still faced with the dressed gluon propagator and the dressed quark-gluon vertex. In principle, the latter is constrained by its Slavnov-Taylor identity [58]

$$k_\nu \Gamma_\nu(q,p) = G(k^2)\left[H(q,p)\, S^{-1}(p) - S^{-1}(q)\, H(q,p)\right] \,, \tag{3.6}$$

where $G(k^2)$ denotes the ghost dressing function and H is an auxiliary function related to the ghost-quark scattering kernel. Unfortunately, the full nonperturbative form of H is still unknown (see [59, 60] for recent work) and one has to employ ansätze for the dressed quark-gluon vertex. Once an ansatz for $\Gamma_\nu(q,p)$ is chosen, one can consider the gluon DSE to obtain the dressed gluon propagator. This equation splits into a pure Yang-Mills part involving only gluons and ghosts (where again truncations are necessary since fully dressed three- and four-gluon vertices appear) and a quark-loop diagram. As a consequence, the gluon and quark DSE have to be solved simultaneously, which is numerically a very hard and demanding task. Furthermore, our goal is the calculation of Taylor coefficients of the quark pressure, which has not been done (at least to our knowledge) before from a Dyson–Schwinger perspective. Thus, we choose a rather simple approximation, the so-called rainbow-ladder (RL) truncation, defined by [54]

$$\frac{1}{8\pi^2} Z_{1\mathrm{F}} g_\mathrm{s}^2\, D_{\mu\nu}(k)\, \Gamma_\nu(q,p) \;\to\; \frac{\alpha_\mathrm{eff}(k^2)}{k^2}\left(\delta_{\mu\nu} - \frac{k_\mu k_\nu}{k^2}\right)\gamma_\nu \,. \tag{3.7}$$

In other words, the RL truncation replaces the dressed gluon propagator and the dressed quark-gluon vertex with their bare values and introduces an effective quark-gluon coupling α_eff. The latter is phenomenologically motivated and constrained by providing an infrared strength sufficient for dynamical chiral symmetry breaking and reproducing the behaviour of the perturbative running coupling of QCD for large momenta. Furthermore, since $Z_{1\mathrm{F}}$ cannot be calculated nonperturbatively without analysing the DSE for the dressed quark-gluon vertex, it is absorbed in the effective coupling. We follow Ref. [61] and use

$$\frac{\alpha_\mathrm{eff}(k^2)}{k^2} := \frac{D}{\omega^4}\, \mathrm{e}^{-k^2/\omega^2} + \frac{\gamma_\mathrm{m}}{k^2 \log\left[\tau + \left(1 + k^2/\Lambda^2_\mathrm{QCD}\right)^2\right]}\left(1 - \mathrm{e}^{-k^2/(4m_\mathrm{t}^2)}\right) \tag{3.8}$$

	m_π [GeV]	f_π [GeV]	m_K [GeV]	f_K [GeV]
Calculation	0.136	0.090	0.497	0.110
Experiment	0.138	0.092	0.496	0.113

Table 3.1.: Masses and decay constants of pions and kaons obtained from a Dyson–Schwinger and Bethe–Salpeter calculation with the model of Eq. (3.8) [61]. The experimental values are taken from Ref. [62].

with

$$\begin{aligned} \gamma_\mathrm{m} &= \frac{12}{25}\,, \qquad \tau = \mathrm{e}^2 - 1\,, \\ \Lambda_\mathrm{QCD} &= 0.234\,\mathrm{GeV}\,, \qquad m_\mathrm{t} = 0.5\,\mathrm{GeV}\,. \end{aligned} \tag{3.9}$$

Furthermore, we choose

$$(D\omega)^{1/3} = 0.8\,\mathrm{GeV} \tag{3.10}$$

with $\omega = 0.6\,\mathrm{GeV}$ (we refer to [61] for more information). Together with current-quark masses $m_\mathrm{u}(\zeta) = m_\mathrm{d}(\zeta) = 3.4\,\mathrm{MeV}$ for up and down quarks, $m_\mathrm{s}(\zeta) = 82\,\mathrm{MeV}$ for the strange quark at a renormalisation point of $\zeta = 19\,\mathrm{GeV}$, the model described by Eq. (3.8) yields a good description of pion and kaon masses and their decay constants (cf. Table 3.1). The effective coupling α_eff with the above described parameters is shown in Figure 3.1.

With the RL truncation, all quantities in the qDSE are specified. Thus, we obtained a closed integral equation which is diagrammatically given by

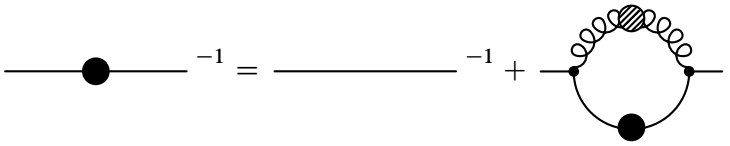

(3.11)

where the shaded dot denotes a bare gluon mediating the effective coupling. Now, the RL-truncated qDSE has to be solved numerically. To this end, the inverse dressed quark propagator is parameterised in Dirac space by

$$S^{-1}(p) = -\mathrm{i}\not{p}\,A(p^2) + B(p^2)\,, \tag{3.12}$$

where A and B are the vector and scalar dressing functions, respectively. They are nontrivial functions of p^2 and incorporate the full nonperturbative nature of the dressed quark propagator. Inverting (3.12) in Dirac space yields

$$S(p) = \frac{\mathrm{i}\not{p}\,A(p^2) + B(p^2)}{p^2 A^2(p^2) + B^2(p^2)}\,, \tag{3.13}$$

which is often written as

$$S(p) = Z(p^2)\,\frac{\left(-\mathrm{i}\not{p} + M(p^2)\right)}{p^2 + M^2(p^2)}\,, \tag{3.14}$$

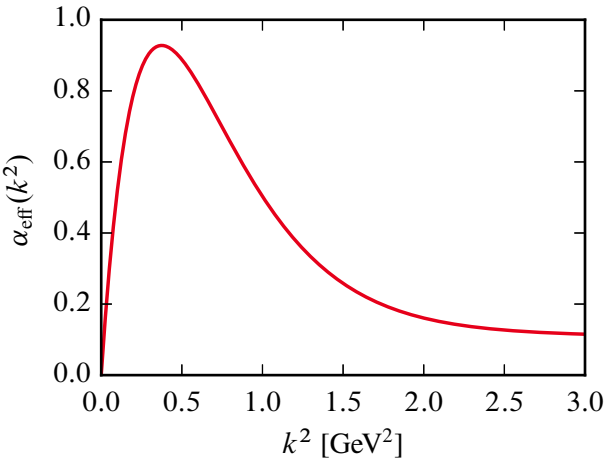

Figure 3.1.: Effective coupling obtained from Eq. (3.8) with parameters as described in (3.9) and (3.10), where $\omega = 0.6\,\text{GeV}$.

where $Z(p^2) := 1/A(p^2)$ and $M(p^2) := B(p^2)/A(p^2)$ are the quark wave function and quark mass function, respectively. Thus, the RL-truncated qDSE reads

$$\begin{aligned} -\mathrm{i}\not{p}A(p^2) + B(p^2) = Z_2\left(-\mathrm{i}\not{p} + Z_m m_f\right) + \frac{32\pi^2}{3}\int \frac{\mathrm{d}^4 q}{(2\pi)^4}\frac{\alpha_{\text{eff}}(k^2)}{k^2} \\ \times\ \gamma_\mu\left(\delta_{\mu\nu} - \frac{k_\mu k_\nu}{k^2}\right)\frac{\mathrm{i}\not{q}A(q^2) + B(q^2)}{q^2A^2(q^2) + B^2(q^2)}\,\gamma_\nu \end{aligned} \tag{3.15}$$

Solving this equation now means solving for the dressing functions A and B. Before doing that, we evaluate the Dirac structure of the integral kernel. Using the relations (A.9), we find

$$\gamma_\mu\left(\delta_{\mu\nu} - \frac{k_\mu k_\nu}{k^2}\right)S(q)\,\gamma_\nu = \frac{1}{q^2A^2(q^2) + B^2(q^2)}\left[-\mathrm{i}\left(\not{q} + 2\frac{k\cdot q}{k^2}\not{k}\right)A(q^2) + 3B(q^2)\right]. \tag{3.16}$$

In order to obtain equations determining the dressing functions A and B, we project the qDSE (3.15) onto them. The projections are given by

$$A(p^2) = -\frac{1}{4\mathrm{i}p^2}\,\mathrm{Tr}\left[\not{p}S^{-1}(p)\right], \tag{3.17a}$$

$$B(p^2) = \frac{1}{4}\,\mathrm{Tr}\left[S^{-1}(p)\right]. \tag{3.17b}$$

Carrying out the projections, we arrive at the following coupled integral equations for the dressing

functions A and B:

$$A(p^2) = Z_2 + \frac{32\pi^2}{3p^2} \int \frac{\mathrm{d}^4 q}{(2\pi)^4} \frac{\alpha_{\mathrm{eff}}(k^2)}{k^2} \left(2\,\frac{(k\cdot q)(p\cdot k)}{k^2} + p\cdot q \right) \frac{A(q^2)}{q^2 A^2(q^2) + B^2(q^2)} \,, \tag{3.18a}$$

$$B(p^2) = Z_2 Z_m m_f + 32\pi^2 \int \frac{\mathrm{d}^4 q}{(2\pi)^4} \frac{\alpha_{\mathrm{eff}}(k^2)}{k^2} \frac{B(q^2)}{q^2 A^2(q^2) + B^2(q^2)} \,. \tag{3.18b}$$

3.1.2. Numerical Method and Renormalisation

In order to solve the obtained equations (3.18a) and (3.18b), we simplify them further using hyperspherical coordinates

$$\int \frac{\mathrm{d}^4 q}{(2\pi)^4} = \frac{1}{8\pi^3} \int_{\varepsilon^2}^{\Lambda^2} \mathrm{d}y\, y \int_{-1}^{1} \mathrm{d}z\, \sqrt{1-z^2} \,, \tag{3.19}$$

where $y := q^2$, $z := \cos(\vartheta(p,q)) = p\cdot q \,/\, \sqrt{p^2 q^2}$, and two trivial angular dependencies are already integrated out. Furthermore, we introduced an ultraviolet (UV) cutoff Λ and an infrared (IR) cutoff ε for the radial integration. The latter is chosen small enough that its effect is negligible and the dependence on Λ will be removed by the renormalisation procedure, which will be explained later. With $x := p^2$, the final form of the equations for the dressing functions reads

$$\begin{aligned} A(x) = Z_2 + \frac{4}{3\pi}\frac{1}{\sqrt{x}} \int_{\varepsilon^2}^{\Lambda^2} \mathrm{d}y \int_{-1}^{1} \mathrm{d}z\, \sqrt{1-z^2}\, \frac{\alpha_{\mathrm{eff}}\big(x+y-2\sqrt{xy}\,z\big)}{x+y-2\sqrt{xy}\,z} \\ \times \left[2\,\frac{\big(\sqrt{x}\,z-\sqrt{y}\big)\big(\sqrt{x}-\sqrt{y}\,z\big)}{x+y-2\sqrt{xy}\,z} + z \right] \frac{y^{3/2} A(y)}{yA^2(y) + B^2(y)} \end{aligned} \tag{3.20a}$$

and

$$B(x) = Z_2 Z_m m_f + \frac{4}{\pi} \int_{\varepsilon^2}^{\Lambda^2} \mathrm{d}y \int_{-1}^{1} \mathrm{d}z\, \sqrt{1-z^2}\, \frac{\alpha_{\mathrm{eff}}\big(x+y-2\sqrt{xy}\,z\big)}{x+y-2\sqrt{xy}\,z} \frac{yB(y)}{yA^2(y) + B^2(y)} \,. \tag{3.20b}$$

We solve these equations self-consistently by iteration, where the iteration process is specified as follows:

(1) Choose initial values for A and B.

(2) Evaluate the right hand side of (3.20a) and (3.20b).

(3) Check if the right hand side and left hand side of (3.20a) and (3.20b) are equal within the desired accuracy.

(4) If the desired accuracy is not achieved yet, goto step two with the newly obtained values for A and B. Otherwise, the iteration process is finished and we found a self-consistent solution (within the desired accuracy) of the Eqs. (3.20a) and (3.20b).

To implement this iterative procedure, the dressing functions are discretised on a momentum grid, which points are logarithmically distributed. This leads to the question how the occuring integrals are treated numerically. A generic integral is usually written as a so-called weighted N-point quadrature rule given by [63, 64]

$$\int_a^b \mathrm{d}x\, f(x)\, W(x) = \sum_{i=1}^{N} w_i\, f(x_i) + R_{N+1}[f]\,. \tag{3.21}$$

The integral of f multiplied by some weight function W is written as a weighted sum over particular function values $f(x_i)$ added by a remainder R_{N+1}. The w_i's and x_i's are called integration weights and integration nodes, respectively. In practical calculations, N is chosen sufficiently large and the remainder is neglegted. For the radial integrals in Eqs. (3.20a) and (3.20b) we use a standard N_{rad}-point Gauss–Legendre quadrature, whereas the angular integrals are done via an N_{ang}-point Gauss–Chebyshev quadrature. The reason for the latter is the appearance of the weight function $W(z) = \sqrt{1-z^2}$ for the angular integrals. An overview about these quadrature rules can be found in [65].

We use an IR cutoff of $\varepsilon = 1\,\mathrm{MeV}$, an UV cutoff of $\Lambda = 1\,\mathrm{TeV}$, $N_{\mathrm{rad}} = 500$ Gauss–Legendre nodes, and $N_{\mathrm{ang}} = 100$ Gauss–Chebyshev nodes. The grid on that the dressing function are discretised is exactly the Gauss–Legendre grid for the radial integrations. Furthermore, the initial values for the dressing functions are $A(x_i) = 1$ and $B(x_i) = 1\,\mathrm{GeV}$, where $i = 1, \ldots, N_{\mathrm{rad}}$. The termination condition for the iteration is a relative error of the dressing functions from the current iteration step compared to the dressing functions from previous iteration step of less than 10^{-6} at each grid point.

Before we discuss the renormalisation, we would like to mention that the qDSE has more than one solution (see [66] for a detailed discussion in three-dimensional QED). For example, $B(x) = 0$ solves Eq. (3.20b) for $m_f = 0$ (chiral limit) and we are left with only one equation for the vector dressing function A. Which solution is obtained via the iteration method depends on the initial values. The solution $B(x) = 0$ is only obtained if the initial values for B are exactly zero. Even a very small initial value of 1 eV leads to a convergence towards the solution $B(x) \neq 0$. In principle, one has to determine which solution is physically realised by checking which one minimises the free energy of the system. However, the physically realised solution in the vacuum is $B(x) \neq 0$.

Finally, we are left with the renormalisation procedure. To this end, the equations (3.20a) and

(3.20b) are written as

$$A(x) = Z_2 + \Sigma_A(x) \,, \tag{3.22a}$$

$$B(x) = Z_2 Z_m m_f + \Sigma_B(x) \,, \tag{3.22b}$$

where Σ_A and Σ_B are the vector and scalar self-energy, respectively, which are readily identified by comparison with Eqs. (3.20a) and (3.20b). In renormalising we require that

$$S^{-1}(p)\big|_{p^2=\zeta^2} \stackrel{!}{=} \left(-\mathrm{i}\not{p} + m_f\right)\big|_{p^2=\zeta^2} \tag{3.23}$$

at the renormalisation point ζ. The renormalisation is performed using a momentum-subtraction scheme [67, 68]. Thus, we isolate Z_2 in (3.22a) and subtract the same equation at $x = \zeta^2$. Using the renormalisation condition $A(\zeta^2) = 1$ (cf. Eq. (3.23)), the renormalised vector dressing function reads

$$A(x) = 1 - \Sigma_A(\zeta^2) + \Sigma_A(x) \,, \tag{3.24}$$

which implies that the wave function renormalisation constant is given by

$$Z_2 = 1 - \Sigma_A(\zeta^2) \,. \tag{3.25}$$

Similarly, we find for the renormalised scalar dressing function

$$B(x) = \Sigma_B(x) - \Sigma_B(\zeta^2) + m_f \,, \tag{3.26}$$

where we used the renormalisation condition $B(\zeta^2) = m_f$, yielding

$$Z_m = \frac{1}{Z_2}\left(1 - \frac{\Sigma_B(\zeta^2)}{m_f}\right) \tag{3.27}$$

for the mass renormalisation constant. Note that this holds only for the case $m_f \neq 0$ of explicit chiral symmetry breaking. In the chiral limit ($m_f = 0$), the scalar dressing function is solely given by its self-energy and does not get renormalised.

3.1.3. Results

Now we would like to present the solutions obtained from the equations (3.20a) and (3.20b) with the RL truncation described in Eqs. (3.8), (3.9), and (3.10). The renormalisation point throughout this work is always $\zeta = 19\,\mathrm{GeV}$ and the momentum dependence is expressed in terms of $x = p^2$.

First of all, a necessary check is whether the renormalisation procedure works, i.e. changing the UV cutoff must not alter the dressing functions. Figure 3.2 shows the quark wave function and the quark mass function for different values of the UV cutoff Λ, namely 1 TeV (our default setting) and twice as much, 2 TeV. As expected, the results does not change and the curves match up perfectly. Thus, the renormalisation procedure works as expected and the dressing functions obtained from their integral equations are independent of the UV cutoff.

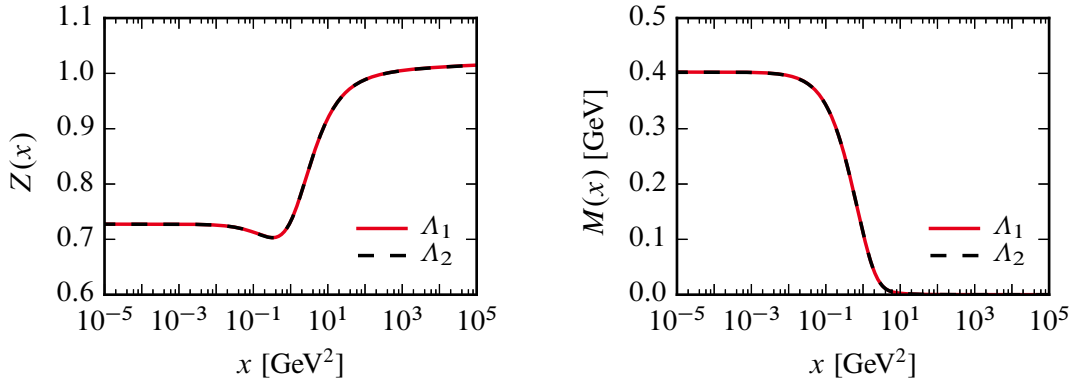

Figure 3.2.: Quark wave function Z (left) and mass function M (right) in the chiral limit for two different UV cutoffs: $\Lambda_1 = 1\,\text{TeV}$ and $\Lambda_2 = 2\,\text{TeV}$.

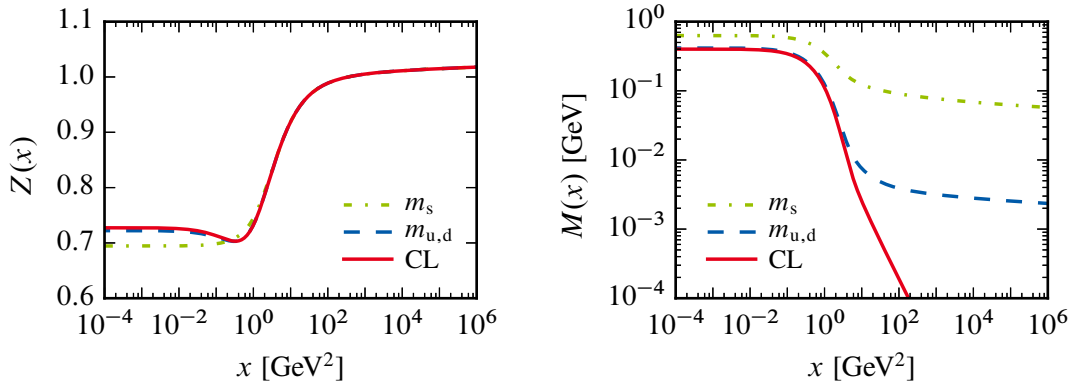

Figure 3.3.: Quark wave function Z (left) and mass function M (right) for current quark masses $m_{u,d} = 3.4\,\text{MeV}$, $m_s = 82\,\text{MeV}$ (fixed at the renormalisation point $\zeta = 19\,\text{GeV}$), and for the chiral limit (denoted by "CL").

In Figure 3.3 we present the quark wave function Z and mass function M for different-current quark masses. Regarding the former, the difference between the chiral limit and a small degenerated mass for up- and down-quarks is visible in the IR only. There, a small quark mass leads to slighty lower values compared to the chiral limit. However, in the momentum region $x \gtrsim 20\,\text{GeV}^2$ the curves become indistinguishable, marking the transition from the nonperturbative to the perturbative domain. Furthermore, we observe that Z acquires values about unity at large momenta, for example $Z(\Lambda^2) \approx 1.017$. This is consistent with perturbation theory, where $Z \equiv 1$. The significantly larger mass of the strange quark alters the shape of Z, where the dip in the region about $x \approx 1\,\text{GeV}^2$ for vanishing and small quark masses does not build up. The quark mass function shows a nontrivial momentum dependence with a significant enhancement in the IR, breaking chiral symmetry dynamically. This applies even to the chiral limit, where the quarks are initially treated as massless. This shows that dynamical chiral symmetry breaking is manifest

in our model and it is the only reason for a non-zero chiral limit solution. The difference between the chiral limit and a small quark mass is barely noticable in the IR but changes at momenta $x \gtrsim 20\,\mathrm{GeV}^2$, marking again the transition from the nonperturbative to the perturbative region. The observed behaviour of Z and M is also found by lattice QCD calculations, see e.g. [69, 70].

3.2. Nonzero Temperature and Density

In the preceding section, we discussed how to solve the qDSE within our RL truncation in the vacuum. Since we would like to compute the temperature-dependent Taylor coefficients of the quark pressure with respect to the chemical potential μ about $\mu = 0$, we have to solve the qDSE in the medium, i.e. at nonzero T and μ.

3.2.1. The Quark Dyson–Schwinger Equation Revisited

The qDSE at nonzero temperature and density is given in Eq. (2.59). Furthermore, the relations (3.4) to reduce it to an equation with only Dirac structure also apply in the medium. Thus, the qDSE reads

$$S(\omega_n, \boldsymbol{p}; \mu) = S_0^{-1}(\omega_n, \boldsymbol{p}; \mu) + \Sigma(\omega_n, \boldsymbol{p}; \mu) \,, \tag{3.28}$$

where the inverse bare propagator is given by

$$S_0^{-1}(\omega_n, \boldsymbol{p}; \mu) = Z_2 \left(-\mathrm{i}\widetilde{\omega}_n \gamma_4 - \mathrm{i}\not{\boldsymbol{p}} + Z_m m_f\right) \tag{3.29}$$

and the self-energy reads

$$\Sigma(\omega_n, \boldsymbol{p}; \mu) = \frac{4}{3} Z_{1\mathrm{F}} g_\mathrm{s}^2 T \sum_{l=-\infty}^{\infty} \int \frac{\mathrm{d}^3\boldsymbol{q}}{(2\pi)^3} \gamma_\nu D_{\nu\rho}(\Omega_{nl}, \boldsymbol{k}) S(\omega_l, \boldsymbol{q}; \mu) \Gamma_\rho(\omega_l, \boldsymbol{q}, \omega_n, \boldsymbol{p}; \mu) \,. \tag{3.30}$$

Recall that $\widetilde{\omega}_n = \omega_n + \mathrm{i}\mu$, $\Omega_{nl} = \omega_n - \omega_l$, and $\boldsymbol{k} = \boldsymbol{p} - \boldsymbol{q}$. In the above equations we made the dependence on the chemical potential μ explicit. However, we will drop this dependency for the sake of brevity from now on.

The most crucial difference compared to the vacuum is the form of the gluon propagator. Since the coupling to heat bath breaks the original O(4) symmetry in the vacuum to O(3) in the medium, the gluon splits into a transversal and longitudinal part with separate dressing functions. Thus, the dressed gluon propagator takes the form

$$D_{\nu\rho}(\Omega_{nl}, \boldsymbol{k}) = \frac{Z_{\mathrm{YM}}^{\mathrm{T}}(k^2)}{k^2} \mathcal{P}_{\nu\rho}^{\mathrm{T}}(k) + \frac{Z_{\mathrm{YM}}^{\mathrm{L}}(k^2)}{k^2} \mathcal{P}_{\nu\rho}^{\mathrm{L}}(k) \,, \tag{3.31}$$

where we defined $k := (\Omega_{nl}, \boldsymbol{k})$; hence $k^2 = \Omega_{nl}^2 + \boldsymbol{k}^2$. Furthermore, $\mathcal{P}^{\mathrm{T}}_{\nu\rho}(k)$ and $\mathcal{P}^{\mathrm{L}}_{\nu\rho}(k)$ denotes the transversal and longitudinal projector, respectively. They are defined by

$$\mathcal{P}^{\mathrm{T}}_{\nu\rho}(k) := \begin{cases} 0 & \text{for } \nu = 4 \text{ and/or } \rho = 4 \,, \\ \delta_{\nu\rho} - \dfrac{k_\nu k_\rho}{\boldsymbol{k}^2} & \text{for } \nu, \rho \in \{1,2,3\} \,, \end{cases} \tag{3.32a}$$

and

$$\mathcal{P}^{\mathrm{L}}_{\nu\rho}(k) := \begin{cases} \delta_{\nu\rho} - \dfrac{k_\nu k_\rho}{k^2} & \text{for } \nu = 4 \text{ and/or } \rho = 4 \,, \\ \dfrac{\Omega_{nl}^2}{\boldsymbol{k}^2} \dfrac{k_\nu k_\rho}{k^2} & \text{for } \nu, \rho \in \{1,2,3\} \,. \end{cases} \tag{3.32b}$$

Consequently, the RL truncation in the medium reads

$$\begin{aligned} &\Gamma_\rho(\omega_l, \boldsymbol{q}, \omega_n, \boldsymbol{p}) \;\to\; \gamma_\rho \,, \\ &\frac{1}{8\pi^2} Z_{1\mathrm{F}} g_{\mathrm{s}}^2 D_{\nu\rho}(k) \;\to\; \frac{1}{k^2} \left[\alpha^{\mathrm{T}}_{\mathrm{eff}}(k^2) \mathcal{P}^{\mathrm{T}}_{\nu\rho}(k) + \alpha^{\mathrm{L}}_{\mathrm{eff}}(k^2) \mathcal{P}^{\mathrm{L}}_{\nu\rho}(k) \right] , \end{aligned} \tag{3.33}$$

with a transversal and longitudinal effective interaction $\alpha^{\mathrm{T}}_{\mathrm{eff}}$ and $\alpha^{\mathrm{L}}_{\mathrm{eff}}$, respectively. In general, they do not have to be equal.

The parametrisation of the quark propagator in Dirac space in the medium is closely related to its counterpart in vacuum (Eq. (3.12)). The broken O(4) symmetry due to the heat bath is reflected in the appearance of a third dressing function. Thus, we write

$$S^{-1}(\omega_n, \boldsymbol{p}) = -\mathrm{i}\widetilde{\omega}_n \gamma_4 C(\omega_n, \boldsymbol{p}^2) - \mathrm{i}\not{\boldsymbol{p}} A(\omega_n, \boldsymbol{p}^2) + B(\omega_n, \boldsymbol{p}^2) \,, \tag{3.34}$$

where the scalar functions C, A, and B are referred to as the temporal, vector, and scalar dressing function, respectively. They are complex valued but purely real for vanishing chemical potential. Inverting (3.34) yields

$$S(\omega_n, \boldsymbol{p}) = \mathrm{i}\widetilde{\omega}_n \gamma_4 \mathcal{D}_C(\omega_n, \boldsymbol{p}^2) + \mathrm{i}\not{\boldsymbol{p}} \mathcal{D}_A(\omega_n, \boldsymbol{p}^2) + \mathcal{D}_B(\omega_n, \boldsymbol{p}^2) \,, \tag{3.35}$$

where we defined for convenience

$$\mathcal{D}_F(\omega_n, \boldsymbol{p}^2) := \frac{F(\omega_n, \boldsymbol{p}^2)}{\widetilde{\omega}_n^2 C^2(\omega_n, \boldsymbol{p}^2) + \boldsymbol{p}^2 A^2(\omega_n, \boldsymbol{p}^2) + B^2(\omega_n, \boldsymbol{p}^2)} \tag{3.36}$$

for $F \in \{A, B, C\}$. Due to the form of the gluon propagator in the medium, the self-energy (3.30) splits into an transversal and longitudinal part, too. In RL truncation (3.33), the self-energy reads

$$\Sigma(\omega_n, x) = \frac{32\pi^2}{3} T \sum_{l=-\infty}^{\infty} \int \frac{\mathrm{d}^3 \boldsymbol{q}}{(2\pi)^3} \left(\frac{\alpha^{\mathrm{T}}_{\mathrm{eff}}(k^2)}{k^2} \mathfrak{T} + \frac{\alpha^{\mathrm{L}}_{\mathrm{eff}}(k^2)}{k^2} \mathfrak{L} \right) , \tag{3.37}$$

where

$$\mathfrak{T} := \gamma_\nu \mathcal{P}^{\mathrm{T}}_{\nu\rho}(k)\, S(\omega_l, \boldsymbol{q})\, \gamma_\rho \,, \tag{3.38a}$$

$$\mathfrak{L} := \gamma_\nu \mathcal{P}^{\mathrm{L}}_{\nu\rho}(k)\, S(\omega_l, \boldsymbol{q})\, \gamma_\rho \,. \tag{3.38b}$$

The evaluation of these quantities is straightforward and we find

$$\mathfrak{T} = 2\left[-\mathrm{i}\widetilde{\omega}_l\, \gamma_4\, \mathcal{D}_C(\omega_l, \boldsymbol{q}^2) - \mathrm{i}\,\frac{\boldsymbol{k}\cdot\boldsymbol{q}}{\boldsymbol{k}^2}\, \not{k}\, \mathcal{D}_A(\omega_l, \boldsymbol{q}^2) + \mathcal{D}_B(\omega_l, \boldsymbol{q}^2)\right] \tag{3.39}$$

and

$$\begin{aligned}\mathfrak{L} = {} & \left(1 - \frac{\Omega_{nl}^2}{k^2}\right)\left[\mathrm{i}\widetilde{\omega}_l\, \gamma_4\, \mathcal{D}_C(\omega_l, \boldsymbol{q}^2) - \mathrm{i}\not{q}\, \mathcal{D}_A(\omega_l, \boldsymbol{q}^2) + \mathcal{D}_B(\omega_l, \boldsymbol{q}^2)\right] \\ & - \frac{2\mathrm{i}\,\Omega_{nl}^2}{k^2}\left[\widetilde{\omega}_l \not{k}\, \mathcal{D}_C(\omega_l, \boldsymbol{q}^2) + (\boldsymbol{k}\cdot\boldsymbol{q})\, \gamma_4\, \mathcal{D}_A(\omega_l, \boldsymbol{q}^2)\right] \\ & + \frac{\Omega_{nl}^2}{k^2}\left[-\mathrm{i}\widetilde{\omega}_l\, \gamma_4\, \mathcal{D}_C(\omega_l, \boldsymbol{q}^2) + \mathrm{i}\left(2\,\frac{\boldsymbol{k}\cdot\boldsymbol{q}}{\boldsymbol{k}^2}\not{k} - \not{q}\right)\mathcal{D}_A(\omega_l, \boldsymbol{q}^2) + \mathcal{D}_B(\omega_l, \boldsymbol{q}^2)\right] .\end{aligned} \tag{3.40}$$

Now, analogous to the vacuum, we project the the qDSE onto the dressing functions C, A, and B to obtain equations for them. These projections are given by

$$C(\omega_n, \boldsymbol{p}^2) = -\frac{1}{4\mathrm{i}\widetilde{\omega}_n}\,\mathrm{Tr}\big[\gamma_4\, S^{-1}(\omega_n, \boldsymbol{p})\big] \,, \tag{3.41a}$$

$$A(\omega_n, \boldsymbol{p}^2) = -\frac{1}{4\mathrm{i}\boldsymbol{p}^2}\,\mathrm{Tr}\big[\not{p}\, S^{-1}(\omega_n, \boldsymbol{p})\big] \,, \tag{3.41b}$$

$$B(\omega_n, \boldsymbol{p}^2) = \frac{1}{4}\,\mathrm{Tr}\big[S^{-1}(\omega_n, \boldsymbol{p})\big] \,. \tag{3.41c}$$

Finally, the qDSE at nonzero temperature and density in terms of the quark propagator's dressing functions reads

$$C(\omega_n, \boldsymbol{p}^2) = Z_2 + \Sigma_C(\omega_n, \boldsymbol{p}^2) \,, \tag{3.42a}$$

$$A(\omega_n, \boldsymbol{p}^2) = Z_2 + \Sigma_A(\omega_n, \boldsymbol{p}^2) \,, \tag{3.42b}$$

$$B(\omega_n, \boldsymbol{p}^2) = Z_2 Z_m m_f + \Sigma_B(\omega_n, \boldsymbol{p}^2) \,, \tag{3.42c}$$

where Σ_C, Σ_A, and Σ_B denote the temporal, vector, and scalar self-energy, respectively. They

are given by

$$\begin{aligned}\Sigma_C(\omega_n, \boldsymbol{p}^2) &:= -\frac{1}{4\mathrm{i}\widetilde{\omega}_n}\,\mathrm{Tr}\big[\gamma_4\,\Sigma(\omega_n,\boldsymbol{p})\big] \\ &= \frac{64\pi^2}{3}\frac{T}{\widetilde{\omega}_n}\sum_{l=-\infty}^{\infty}\int\frac{\mathrm{d}^3\boldsymbol{q}}{(2\pi)^3}\frac{1}{k^2}\left\{\alpha_{\mathrm{eff}}^{\mathrm{L}}(k^2)\,\Omega_{nl}\,\frac{\boldsymbol{k}\cdot\boldsymbol{q}}{k^2}\,\mathcal{D}_A(\omega_l,\boldsymbol{q}^2)\right. \\ &\quad\left.+\left[\alpha_{\mathrm{eff}}^{\mathrm{T}}(k^2)-\alpha_{\mathrm{eff}}^{\mathrm{L}}(k^2)\left(\frac{1}{2}-\frac{\Omega_{nl}^2}{k^2}\right)\right]\widetilde{\omega}_l\,\mathcal{D}_C(\omega_l,\boldsymbol{q}^2)\right\}, \qquad (3.43a)\end{aligned}$$

$$\begin{aligned}\Sigma_A(\omega_n, \boldsymbol{p}^2) &:= -\frac{1}{4\mathrm{i}\boldsymbol{p}^2}\,\mathrm{Tr}\big[\not{p}\,\Sigma(\omega_n,\boldsymbol{p})\big] \\ &= \frac{64\pi^2}{3}\frac{T}{\boldsymbol{p}^2}\sum_{l=-\infty}^{\infty}\int\frac{\mathrm{d}^3\boldsymbol{q}}{(2\pi)^3}\frac{1}{k^2}\left\{\alpha_{\mathrm{eff}}^{\mathrm{T}}(k^2)\,\frac{(\boldsymbol{k}\cdot\boldsymbol{q})(\boldsymbol{p}\cdot\boldsymbol{k})}{\boldsymbol{k}^2}\,\mathcal{D}_A(\omega_l,\boldsymbol{q}^2)\right. \\ &\quad+\alpha_{\mathrm{eff}}^{\mathrm{L}}(k^2)\left[\frac{1}{2}\left(1-\frac{\Omega_{nl}^2}{k^2}\right)\mathcal{D}_A(\omega_l,\boldsymbol{q}^2)+\widetilde{\omega}_l\,\Omega_{nl}\,\frac{\boldsymbol{p}\cdot\boldsymbol{k}}{k^2}\,\mathcal{D}_C(\omega_l,\boldsymbol{q}^2)\right. \\ &\quad\left.\left.+\frac{\Omega_{nl}^2}{k^2}\left(\frac{\boldsymbol{p}\cdot\boldsymbol{q}}{2}-\frac{(\boldsymbol{k}\cdot\boldsymbol{q})(\boldsymbol{p}\cdot\boldsymbol{k})}{\boldsymbol{k}^2}\right)\mathcal{D}_A(\omega_l,\boldsymbol{q}^2)\right]\right\}, \qquad (3.43b)\end{aligned}$$

$$\begin{aligned}\Sigma_B(\omega_n, \boldsymbol{q}^2) &:= \frac{1}{4}\,\mathrm{Tr}\big[\Sigma(\omega_n,\boldsymbol{p})\big] \\ &= \frac{32\pi^2}{3}\,T\sum_{l=-\infty}^{\infty}\int\frac{\mathrm{d}^3\boldsymbol{q}}{(2\pi)^3}\,\frac{2\alpha_{\mathrm{eff}}^{\mathrm{T}}(k^2)+\alpha_{\mathrm{eff}}^{\mathrm{L}}(k^2)}{k^2}\,\mathcal{D}_B(\omega_l,\boldsymbol{q}^2)\,. \qquad (3.43c)\end{aligned}$$

Numerical Aspects and Renormalisation

The introduction of nonzero temperature and density also affects the actual numerical treatment of the qDSE. Nonzero chemical potential μ yields complex valued dressing functions with a vanishing imaginary part only if $\mu = 0$. Furthermore, in the self-energies appears a sum over the Matsubara frequencies, which cannot be performed analytically. We use spherical coordinates for the momentum integral and the Matsubara sum together with the integral are regularised in an O(4)-invariant way such that $\omega_l^2 + \boldsymbol{q}^2 \leq \Lambda^2$. Thus,

$$\sum_{l=-\infty}^{\infty}\int\frac{\mathrm{d}^3\boldsymbol{q}}{(2\pi)^3}\;\to\;\frac{1}{8\pi^2}\sum_{l=-N_\omega-1}^{N_\omega}\int_{\varepsilon^2}^{\Lambda^2-\omega_l^2}\mathrm{d}y\,\sqrt{y}\int_{-1}^{1}\mathrm{d}z \qquad (3.44)$$

where $y := \boldsymbol{q}^2$ and $z := \cos(\vartheta(\boldsymbol{p},\boldsymbol{q})) = \boldsymbol{p}\cdot\boldsymbol{q}\,/\sqrt{\boldsymbol{p}^2\boldsymbol{q}^2}$. As in the vacuum, we introduced an IR cutoff ε. The regularisation described above is necessary to restore O(4) invariance at large (i.e. perturbative) momenta as well as in the limit of vanishing temperature. Furthermore, we use a simplified version of the RL truncation in the medium where the transversal and longitudinal effective couplings are chosen to be equal. Thus,

$$\alpha_{\mathrm{eff}}^{\mathrm{T}}(k^2) := \alpha_{\mathrm{eff}}(k^2) \quad \text{and} \quad \alpha_{\mathrm{eff}}^{\mathrm{L}}(k^2) := \alpha_{\mathrm{eff}}(k^2)\,, \tag{3.45}$$

where $\alpha_{\mathrm{eff}}(k^2)$ is simply the vacuum effective coupling, given in Eq. (3.8), but recall that now $k^2 = \Omega_{nl}^2 + \boldsymbol{k}^2$. Eventually, with $x := \boldsymbol{p}^2$, the final form of the qDSE reads

$$C(\omega_n, x) = Z_2 + \Sigma_C(\omega_n, x)\,, \tag{3.46a}$$
$$A(\omega_n, x) = Z_2 + \Sigma_A(\omega_n, x)\,, \tag{3.46b}$$
$$B(\omega_n, x) = Z_2 Z_m m_f + \Sigma_B(\omega_n, x)\,, \tag{3.46c}$$

with the self-energies

$$\Sigma_C(\omega_n, x) = \frac{8}{3}\frac{T}{\widetilde{\omega}_n} \sum_{l=-N_\omega-1}^{N_\omega} \int_{\varepsilon^2}^{\Lambda^2-\omega_l^2} \mathrm{d}y\,\sqrt{y} \int_{-1}^{1} \mathrm{d}z\,\frac{\alpha_{\mathrm{eff}}(s)}{s} \times \left[\left(\frac{1}{2} + \frac{\Omega_{nl}^2}{s}\right)\widetilde{\omega}_l\,\mathcal{D}_C(\omega_l, y) + \frac{\Omega_{nl}\left(\sqrt{xy}\,z - y\right)}{s}\,\mathcal{D}_A(\omega_l, y)\right], \tag{3.47a}$$

$$\Sigma_A(\omega_n, x) = \frac{8}{3}\frac{T}{x} \sum_{l=-N_\omega-1}^{N_\omega} \int_{\varepsilon^2}^{\Lambda^2-\omega_l^2} \mathrm{d}y\,\sqrt{y} \int_{-1}^{1} \mathrm{d}z\,\frac{\alpha_{\mathrm{eff}}(s)}{s} \left\{\frac{\widetilde{\omega}_l\,\Omega_{nl}\left(x - \sqrt{xy}\,z\right)}{s}\,\mathcal{D}_C(\omega_l, y) + \left[\left(1 - \frac{\Omega_{nl}^2}{s}\right)\frac{\left(\sqrt{x}\,z - \sqrt{y}\right)\left(\sqrt{x} - \sqrt{y}\,z\right)}{s - \Omega_{nl}^2} + \frac{1}{2}\,z\right]\sqrt{xy}\,\mathcal{D}_A(\omega_l, y)\right\}, \tag{3.47b}$$

$$\Sigma_B(\omega_n, x) = 4T \sum_{l=-N_\omega-1}^{N_\omega} \int_{\varepsilon^2}^{\Lambda^2-\omega_l^2} \mathrm{d}y\,\sqrt{y} \int_{-1}^{1} \mathrm{d}z\,\frac{\alpha_{\mathrm{eff}}(s)}{s}\,\mathcal{D}_B(\omega_l, y)\,, \tag{3.47c}$$

where $s := \Omega_{nl}^2 + x + y - 2\sqrt{xy}\,z$.

From a numerical point of view, we use the same fixed point iteration method described in Section 3.1 to solve the qDSE at nonzero temperature and density. Since the angular integrals lack a distinct weight function, we use a Gauss–Legendre quadrature for both integrations with $N_{\mathrm{rad}} = 300$ radial and $N_{\mathrm{ang}} = 100$ angular nodes. The cutoffs are identical to those for the vacuum calculation, namely $\varepsilon = 1\,\mathrm{MeV}$ and $\Lambda = 1\,\mathrm{TeV}$, and the initial values for the dressing functions are $C(\omega_n, x_i) = 1$, $A(\omega_n, x_i) = 1$, and $B(\omega_n, x_i) = 1\,\mathrm{GeV}$ for $i = 1, \ldots, N_{\mathrm{rad}}$

and for all n. Due to the regularisation (3.44), a different integration grid is required for each Matsubara frequency. Furthermore, all medium calculations are done with $N_\mathrm{f} = 2$ flavours in the chiral limit.

The renormalisation procedure is analogous to the vacuum since the introduction of nonzero temperature and density does not give rise to new divergences [35, 71]. Our renormalisation condition reads [72]

$$C(\omega_0, \boldsymbol{p}^2)\big|_{\mu=0;\omega_0^2+\boldsymbol{p}^2=\zeta^2} \stackrel{!}{=} 1 \tag{3.48}$$

at the renormalisation point ζ in order to fix Z_2. Thus, the quark wave function renormalisation constant is given by [2]

$$Z_2 = 1 - \Sigma_C\left(\omega_0, \zeta^2 - \omega_0^2\right)\big|_{\mu=0} \,. \tag{3.49}$$

Since we use the rainbow-ladder model from the vacuum, the renormalisation point is also given by $\zeta = 19\,\mathrm{GeV}$

Finally, we would like to mention that the dressing functions obey the symmetry relation

$$F(\omega_n, x) = F^*(\omega_{-n-1}, x) \,, \tag{3.50}$$

where $F \in \{A, B, C\}$. Thus, we have to calculate the dressing functions only for positive Matsubara frequencies.

3.2.2. Matsubara Truncation

In the preceding section we described our numerical setup to solve the qDSE in the medium. However, we haven't specified yet how the Matsubara sum is treated. Its truncation is characterised by the parameter N_ω (cf. Eq. (3.44)), which is temperature dependent. It holds that the smaller the temperature, the larger N_ω and vice versa. In principle, the truncation at a given temperature T is given by

$$N_\omega = \left\lfloor \frac{1}{2}\left(\frac{1}{\pi T}\sqrt{\Lambda^2 - \varepsilon^2} - 1\right)\right\rfloor \,. \tag{3.51}$$

However, the results of the above equation are very large. For example, at $T = 100\,\mathrm{MeV}$ we would have to sum $N_\omega = 1591$ Matsubara frequencies, where for each frequency two integrals must be performed. Since this is numerically not feasible, we proceed as follows: A value of N_ω is sufficient for a given temperature if

$$\max_{n=0,\ldots,N_\omega}\left\{\max_{i=1,\ldots,N_\mathrm{rad}}\left|1 - \frac{F^{(N_\omega)}(\omega_n, x_i)}{F^{(N_\omega+1)}(\omega_n, x_i)}\right|\right\} < \eta \tag{3.52}$$

[2] One can also impose this condition on the vector dressing function A, resulting in $Z_2 = 1 - \Sigma_A(\omega_0, \zeta^2 - \omega_0^2)|_{\mu=0}$. We expect that this has an influence on properties like the chiral transition temperature. However, a way to avoid the ambiguous choice of Z_2 is to compute it in the vacuum (i.e. at $T = \mu = 0$) and use this value in the medium calculations.

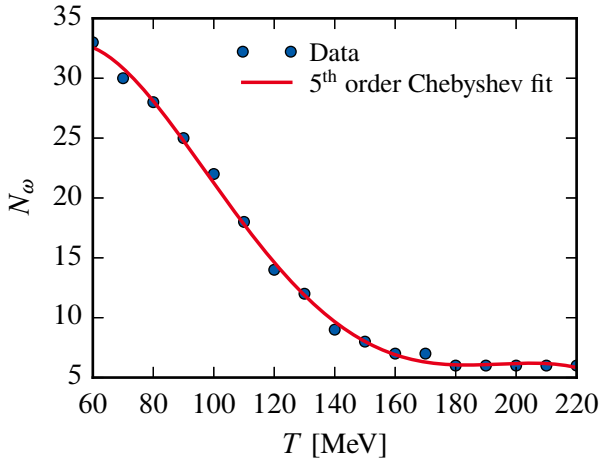

Figure 3.4.: N_ω for different temperatures obtained from (3.52) (blue circles) and a 5$^{\text{th}}$ order Chebyshev fit (Eq. (3.53)).

T [MeV]	220	200	180	160	140	120	100	80	60
N_ω	6	6	6	7	9	14	22	28	33

Table 3.2.: N_ω for different temperatures obtained from (3.52).

holds for $F \in \{A, B, C\}$. Here $F^{(N_\omega)}$ and $F^{(N_\omega+1)}$ denotes that the dressing function was obtained from the qDSE with a Matsubara truncation of N_ω and $N_\omega + 1$, respectively. We choose $\eta = 0.5\,\%$, which is a tradeoff between accuracy and runtime. The results for some distinct temperatures is shown in Table 3.2. To get N_ω for arbitrary temperatures $T/\,\text{MeV} \in [60, 220]$, we fit a 5$^{\text{th}}$ order Chebyshev polynomial

$$f(T) := \sum_{k=0}^{5} a_k \mathcal{T}_k(T) \tag{3.53}$$

to the data points given in Table 3.2, where $\mathcal{T}_k$ denotes the k^{th} Chebyshev polynomial of the second kind. The fit is shown in Figure 3.4. Eventually, we use the Matsubara truncation

$$N_\omega = \lceil f(T) \rceil \tag{3.54}$$

for all $T/\text{MeV} \in [60, 220]$.

3.2.3. Critical Temperature

As already explained in the first chapter, the QCD phase diagram shows a rich phase structure in the (T, μ)-plane. In our case of two quark flavours in the chiral limit, a second-order phase

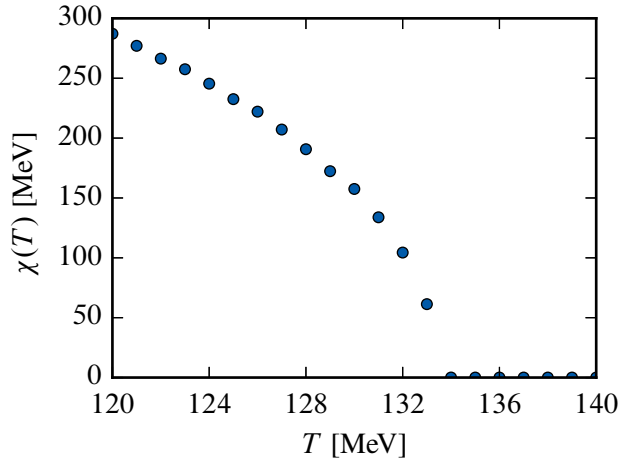

Figure 3.5.: Temperature dependence of the order parameter χ (Eq. (3.55)) for chiral symmetry restoration. It vanishes for temperatures $T \geq 134\,\mathrm{MeV}$.

transition is expected at a distinct temperature for vanishing chemical potential. This so-called critical temperature T_c marks the transition from the phase where chiral symmetry is broken to the phase of restored chiral symmetry along the T-axis for $\mu = 0$. In order to determine the critical temperature, we employ the order parameter [54, 73]

$$\chi(T) := B\big(\omega_0, x = \varepsilon^2\big)\big|_{\mu=0} \,. \tag{3.55}$$

In the chiral symmetric phase ($T \geq T_\mathrm{c}$), χ vanishes whereas it acquires nonzero values in the phase where chiral symmetry is broken ($T < T_\mathrm{c}$). The temperature dependence of the order parameter is shown in Fig. 3.5. The transition is of second order and we find

$$T_\mathrm{c} = 134\,\mathrm{MeV} \,. \tag{3.56}$$

Note that this chiral transition temperature is approximately 15 % smaller compared to recent results from lattice QCD (with $2+1$ flavours) [74]. In principle, this can be resolved by adjusting the parameters of the RL truncation to yield a higher critical temperature. However, this is beyond the scope of this work.

3.2.4. Exemplary Solutions

In Figure 3.6 we present the results for the dressed quark propagator in the medium in terms of its dressing functions. All momentum dependencies are expressed in terms of $x = \boldsymbol{p}^2$.

First we consider the dressing functions C and A at vanishing chemical potential. In Figure 3.6 (a) and (b) these functions are shown for temperatures below T_c, i.e. in the phase where chiral symmetry is broken (i.e. $B \neq 0$). Different temperatures are visible in the IR only and the

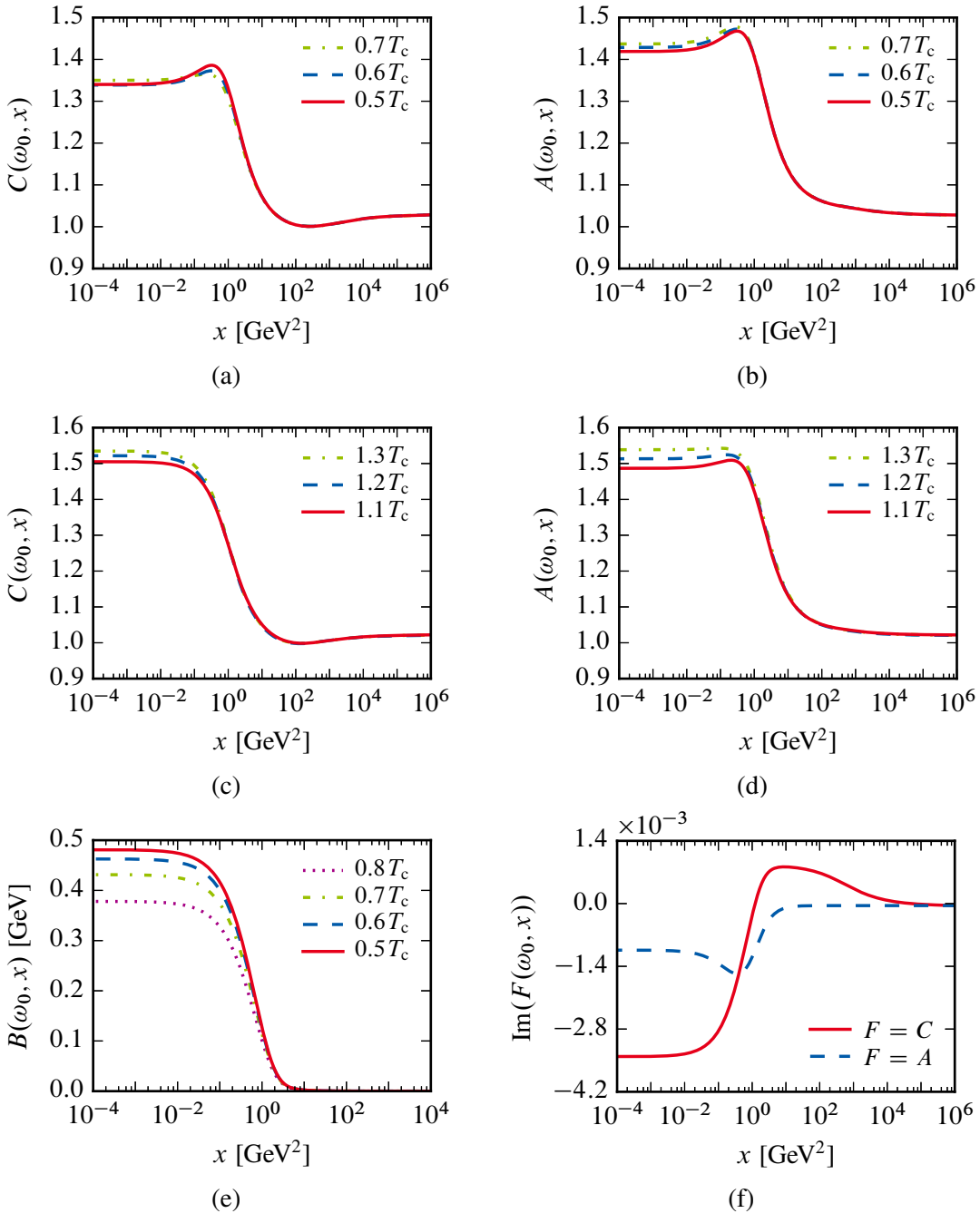

Figure 3.6.: In (a) to (d) we show the functions C and A below (first row) and above (second row) T_c at $\mu = 0$ for the zeroth Matsubara frequency, (e) shows $B(\omega_0, x)$ for various temperatures below T_c at $\mu = 0$, and in (f) we present $\mathrm{Im}(C(\omega_0, x))$ and $\mathrm{Im}(A(\omega_0, x))$ at $T = 1.5\,T_c$ and $\mu = 5\,\mathrm{MeV}$.

functions show no temperature dependence for squared momenta $x \gtrsim 10\,\mathrm{GeV}^2$. Regarding the C function, the difference between $0.5\,T_\mathrm{c}$ and $0.6\,T_\mathrm{c}$ is only marginally visible in the IR, whereas a temperature of $0.7\,T_\mathrm{c}$ yields a slightly larger value in the infrared. The bump in the region about $1\,\mathrm{GeV}^2$ decreases for higher temperatures. The IR-values of A increase with the temperature as well as the bump about $1\,\mathrm{GeV}^2$. In the deep UV, both functions acquire values about unity and become degenerate, e.g. $C\left(\omega_0, \Lambda^2 - \omega_0^2\right) = A\left(\omega_0, \Lambda^2 - \omega_0^2\right) \approx 1.028$, indicating restoration of the O(4) symmetry. Above T_c where chiral symmetry is restored (Figure 3.6 (c) and (d)), the higher the temperature the higher the infrared values of C and A. Furthermore, the bump about $1\,\mathrm{GeV}^2$ of both functions vanishes with increasing temperature. Again, values about unity are acquired in the deep UV and C and A are degenerate.

In Figure 3.6 (e) we present $B(\omega_0, x)$ for different temperatures below the chiral phase transition, where it is nonzero. It shows a nontrivial momentum dependence with values different from zero in the IR, i.e. the quarks acquire a significantly amount of mass in the infrared, breaking chiral symmetry. Above squared momenta of $x \gtrsim 30\,\mathrm{GeV}^2$, B drops to zero. Concerning the temperature dependence, the higher the temperature the smaller the values of B, showing the beginning of chiral symmetry restoration. This is consistent with $\lim_{T \to T_\mathrm{c}} B(\omega_n, x) = 0$.

Finally, Figure 3.6 (f) shows the imaginary parts of $C(\omega_0, x)$ and $A(\omega_0, x)$ at $T = 1.5\,T_\mathrm{c}$ and $\mu = 5\,\mathrm{MeV}$. Since we have a nonzero chemical potential, the imaginary parts do not vanish. There are two features we would like to emphasise. First, the overall scale of the imaginary parts is at least one magnitude smaller compared to the bare values $\mathrm{Re}(C) = \mathrm{Re}(A) = 1$. Second, we observe a bump in the UV of $\mathrm{Im}(C)$, whereas $\mathrm{Im}(A)$ goes to zero for squared momenta $x \gtrsim 25\,\mathrm{GeV}^2$. That behaviour of $\mathrm{Im}(C)$ is contrary to the fact that the medium dominantly affects the infrared. We find that the bump scales with the chemical potential. Furthermore, we observed that if the UV cutoff is changed, the bump changes as well. This characterises it as a numerical artefact and is thus unphysical. The described behaviour of the imaginary part of the temporal dressing function at nonzero chemical potential was also found in Ref. [75]. There it was observed that only the introduction of separate cutoffs for the Matsubara sum and the three-momentum integral cures the problematic behaviour of $\mathrm{Im}(C)$. However, we follow [75] and ignore this numerical artefact, since the scale of the imaginary parts is small compared to the corresponding real parts. [3]

[3] In the process of finishing this work, it came to our attention that the behaviour of $\mathrm{Im}(C)$ in the UV can be fixed if one treats the real and imaginary parts of the dressing functions differently during the regularisation [76].

4. Taylor Coefficients of the Quark Pressure

Up to this point, we solved the quark Dyson–Schwinger equation in vacuum as well as in the medium. In this chapter, we will make contact to thermodynamics to obtain an equation which determines the pressure $\wp$ originating from dressed quarks and from this we get the Taylor coefficients of the pressure with respect to the chemical potential μ about $\mu = 0$.

4.1. The Quark Pressure

All thermodynamic properties of QCD at a temperature T and chemical potential μ are encoded in the grand canonical potential per volume V. It is defined by

$$\Omega(T,\mu) := -\frac{T}{V}\log(\mathcal{Z}(T,\mu)) \,, \tag{4.1}$$

where $\mathcal{Z}(T,\mu)$ is the grand canonical partition function of QCD and given in the path-integral formalism by

$$\mathcal{Z}(T,\mu) := \int \mathcal{D}\big[\bar{\psi}\psi A c \bar{c}\big] \exp\left\{ -\int_0^{1/T} \mathrm{d}x_4 \int \mathrm{d}^3\boldsymbol{x} \left(\mathcal{L}_{\mathrm{gf,R}} + \mu\bar{\psi}\gamma_4\psi \right) \right\} . \tag{4.2}$$

Recall that $\mathcal{L}_{\mathrm{gf,R}}$ is the renormalised and gauge-fixed QCD Lagrangian (see Eq. (2.32)). Having the grand canonical potential defined as above, the pressure is given by

$$\wp(T,\mu) = -\Omega(T,\mu) \,. \tag{4.3}$$

Now we expand the pressure in a Taylor series with respect to the chemical potential about zero, yielding

$$\wp(T,\mu) = \sum_{k=0}^{\infty} d_k(T)\,\mu^k \tag{4.4}$$

with the temperature dependent coefficients

$$d_k(T) := \frac{1}{k!}\frac{\partial^k \wp(T,\mu)}{\partial\mu^k}\bigg|_{\mu=0} . \tag{4.5}$$

Note that since the pressure is of dimension (energy)^4, the coefficients $d_k(T)$ are dimensionful quantities as well with dimension (energy)$^{4-k}$. However, it is more common to use the so-called reduced pressure defined by

$$\bar{\wp}(T,\mu) := \frac{\wp(T,\mu)}{T^4} \,, \tag{4.6}$$

which is now a dimensionless quantity with Taylor expansion

$$\bar{\wp}(T,\mu) = \sum_{k=0}^{\infty} c_k(T) \left(\frac{\mu}{T}\right)^k \tag{4.7}$$

with expansion coefficients

$$c_k(T) := \frac{1}{k!} \frac{\partial^k \bar{\wp}(T,\mu)}{\partial(\mu/T)^k}\bigg|_{\mu=0} \,. \tag{4.8}$$

Consequently, the coefficients (4.5) and (4.8) are related by $c_k(T) = T^{k-4}\, d_k(T)$.

In principle, the Taylor coefficients of the pressure can now be obtained from Eq. (4.3) via μ-derivatives. Unfortunately, the partition function cannot be calculated analytically and the equation for the pressure is therefore impractical from a computational point of view. Thus, we choose an approach based on the two-particle irreducible (2PI) effective action Γ_{2PI}. It is obtained by a Legendre transform of the 1PI effective action (2.24), which is itself a Legendre transform of the generating functional for connected correlations functions (see Section 2.1.3). Therefore, Γ_{2PI} depends on the one- and two-point functions of the theory. In general, it contains a gluonic, a ghost, and a quark part. One particular useful feature of the 2PI effective action is that it can be related to the thermodynamic potential and hence to the pressure. Since we are interested in the quark pressure, we need only the quark contribution to the 2PI effective action. It is given by [77, 78]

$$\Gamma_{\text{2PI}}[S] = \operatorname{Tr}\log\frac{S^{-1}}{T} - \operatorname{Tr}\big[\mathbb{1} - S_0^{-1}S\big] + \Gamma_{\text{int}}[S] \,, \tag{4.9}$$

where S is the dressed and S_0 the bare quark propagator. Furthermore, Γ_{int} incorporates the interaction and is given by a sum of all 2PI diagrams with respect to S. Note that we do not include a field dependence in terms of macroscopic quark fields, since quarks do not acquire nonzero expectation values due to their Grassmann nature. Furthermore, the traces in (4.9) are meant in the functional sense, i.e. they run over flavour, colour, Dirac, and momentum space. The connection to thermodynamics is established by the relation

$$\frac{V}{T}\,\Omega(T,\mu) = -\Gamma_{\text{2PI}}\Big|_{\text{stat. pt.}} \,, \tag{4.10}$$

i.e. the 2PI effective action evaluated at the stationary point (indicated by "$|_{\text{stat. pt.}}$") equals, up to the four-volume factor V/T, the negative thermodynamic potential. Thus, the quark pressure is

given by

$$\begin{aligned} \wp(T,\mu) &= \left.\frac{T}{V}\,\Gamma_{\mathrm{2PI}}\right|_{\text{stat. pt.}} \\ &= \left.\frac{T}{V}\left(\operatorname{Tr}\log\frac{S^{-1}}{T} - \operatorname{Tr}\left[\mathbb{1} - S_0^{-1}S\right] + \Gamma_{\mathrm{int}}[S]\right)\right|_{\text{stat. pt.}} . \end{aligned} \tag{4.11}$$

The stationary point of the 2PI effective action is obtained by extremising it with respect to the dressed quark propagator, viz.

$$\frac{\delta\Gamma_{\mathrm{2PI}}[S]}{\delta S} \stackrel{!}{=} 0 \,. \tag{4.12}$$

Carrying out the derivative, we arrive at the qDSE

$$S^{-1} = S_0^{-1} + \Sigma \tag{4.13}$$

with the quark self-energy

$$\Sigma = \frac{\delta\Gamma_{\mathrm{int}}}{\delta S} \,. \tag{4.14}$$

In other words, the evaluation of the quark pressure via the 2PI effective action at its stationary point means that the dressed quark propagator S has to obey the DSE (4.13). In general, it is always possible to derive a DSE from a given effective action. However, not every DSE allows an explicit construction of its generating 2PI effective action, as it is not always possible to solve Eq. (4.14) explicitly for Γ_{int}.

In order to proceed, the interaction part must be chosen such that (4.14) yields the RL-truncated self-energy (3.37). It follows that Γ_{int} is given by

$$\begin{aligned} \Gamma_{\mathrm{int}}[S] &= \frac{1}{2} \\ &= \frac{1}{2}\operatorname{Tr}[\Sigma S] \\ &= \frac{1}{2}\operatorname{Tr}\left[\mathbb{1} - S_0^{-1}S\right] , \end{aligned} \tag{4.15}$$

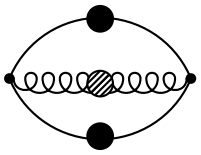

where the last equality follows from the qDSE (4.13). Note that this is only valid at the stationary point. Since functional differentiation with respect to S corresponds diagrammatically to opening an internal quark line, we find indeed

$$\frac{\delta}{\delta S}\left\{\frac{1}{2}\right. \left.\right\} =$$.

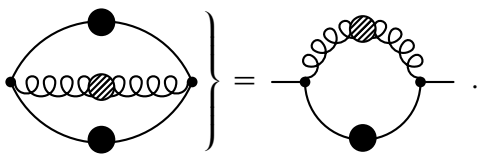

(4.16)

Note that the form (4.15) of Γ_{int} is also valid beyond RL truncation as long as the dressed gluon and the dressed quark-gluon vertex are independent of the quark propagator. With Γ_{int} specified as above, the quark pressure reads

$$\wp(T,\mu) = \frac{T}{V}\left(\operatorname{Tr}\log\frac{S^{-1}}{T} - \frac{1}{2}\operatorname{Tr}\left[\mathbb{1} - S_0^{-1}S\right]\right), \tag{4.17}$$

where the dressed quark propagator S is the solution of the qDSE (3.28) in RL truncation. As already mentioned, the traces have to be taken in momentum, flavour, colour, and Dirac space. Since we use two flavours in the chiral limit, the flavour trace yields simply a factor of $N_{\text{f}} = 2$. The same holds for the colour trace, contributing a factor of $N_{\text{c}} = 3$ since S is diagonal in colour space. Furthermore, the trace in momentum space consists of a sum over all Matsubara frequencies and all three-momenta,

$$\operatorname{Tr}_{\text{momentum}} \equiv \sum_{\omega_l}\sum_{\boldsymbol{q}}, \tag{4.18}$$

since the dressed quark propagator is diagonal in these spaces as well. The three-momentum sum is given in the infinite-volume limit by

$$\sum_{\boldsymbol{q}} \to V\int\frac{\mathrm{d}^3\boldsymbol{q}}{(2\pi)^3}. \tag{4.19}$$

The above assumptions that the dressed quark propagator is diagonal in colour and momentum space is at least valid in the region of the phase diagram we are concerned with. The situation is different, for example, in colour-superconducting phases (see, e.g. [79]).

Eventually, we arrive at the final form of the quark pressure

$$\wp(T,\mu) = 6T\sum_{l=-\infty}^{\infty}\int\frac{\mathrm{d}^3\boldsymbol{q}}{(2\pi)^3}\left(\operatorname{Tr}\log\frac{S^{-1}(\omega_l,\boldsymbol{q})}{T} - \frac{1}{2}\operatorname{Tr}\left[\mathbb{1} - S_0^{-1}(\omega_l,\boldsymbol{q})\,S(\omega_l,\boldsymbol{q})\right]\right), \tag{4.20}$$

where the traces are now over Dirac degrees of freedom only. This equation is the starting point to derive equations for the Taylor coefficients by subsequent derivatives with respect to μ.

4.2. Derivatives of the Dressing Functions

As apparent from Eq. (4.20), a derivative of $\wp$ with respect to the chemical potential results in derivatives of the quark propagator and thus in derivatives of the dressing functions with respect to μ which must then be evaluated at $\mu = 0$. Additionally to the symmetry (3.50), the dressing functions obey $F(\omega_n, x; \mu) = F^*(\omega_n, x; -\mu)$, $F \in \{A, B, C\}$, i.e.

$$\begin{aligned}\operatorname{Re}(F(\omega_n,x;\mu)) &= \operatorname{Re}(F(\omega_n,x;-\mu)),\\ \operatorname{Im}(F(\omega_n,x;\mu)) &= -\operatorname{Im}(F(\omega_n,x;-\mu)),\end{aligned} \tag{4.21}$$

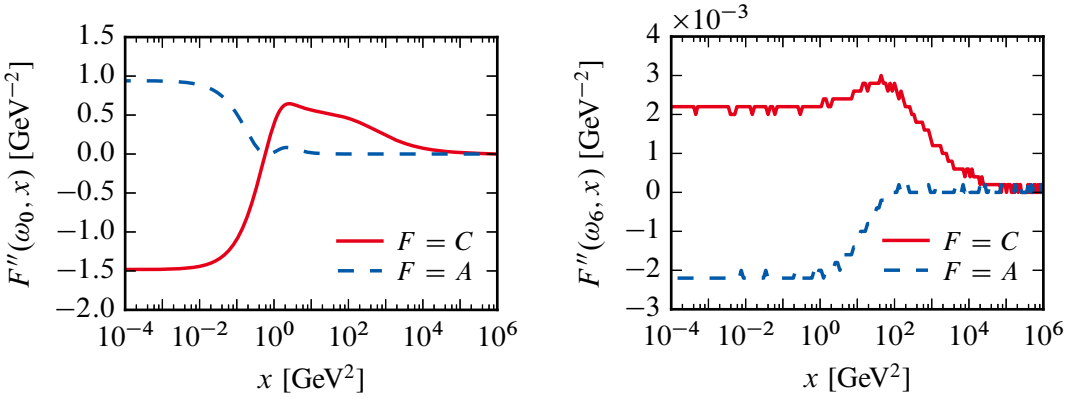

Figure 4.1.: Second μ-derivative of the dressing functions C and A at temperature $T = 1.5\,T_\mathrm{c}$ according to (4.23) with $\mu = 1\,\mathrm{MeV}$. Shown are results for the zeroth (left) and sixth (right) Matsubara frequency.

where we made the dependence on the chemical potential explicit [1]. Furthermore, recall that $x = \boldsymbol{p}^2$. In other words, the real part of the dressing functions is symmetric whereas the imaginary part is antisymmetric with respect to μ. Therefore, it follows that

$$\left.\frac{\partial^k F(\omega_n, x)}{\partial \mu^k}\right|_{\mu=0} = \begin{cases} \left.\dfrac{\partial^k \operatorname{Re}(F(\omega_n, x))}{\partial \mu^k}\right|_{\mu=0} & \text{for } k \in \{2, 4, 6, \ldots\}\,, \\ \mathrm{i}\left.\dfrac{\partial^k \operatorname{Im}(F(\omega_n, x))}{\partial \mu^k}\right|_{\mu=0} & \text{for } k \in \{1, 3, 5, \ldots\}\,. \end{cases} \tag{4.22}$$

Our first approach to the derivatives of the dressing functions is a simple difference quotient. For example, the central difference quotient for the second derivative reads [65]

$$\begin{aligned} F''(\omega_n, x) &:= \left.\frac{\partial^2 F(\omega_n, x)}{\partial \mu^2}\right|_{\mu=0} \\ &\approx \frac{2}{\mu^2}\left[\operatorname{Re}(F(\omega_n, x; \mu)) - \operatorname{Re}(F(\omega_n, x; 0))\right], \end{aligned} \tag{4.23}$$

where we already exploited the symmetry (4.21). Note that μ must be chosen sufficiently small since it is used as the step size for the difference quotient. In Figure 4.1 we present the second derivatives of C and A according to (4.23) at $T = 1.5\,T_\mathrm{c}$ for the zeroth and sixth Matsubara frequency. The difference quotient is calculated with $\mu = 1\,\mathrm{MeV}$. The results for the zeroth Matsubara frequency (left panel in Figure 4.1) are smooth but numerical artefacts increase for higher Matsubara frequencies (right panel in Figure 4.1) and the difference quotient becomes

[1] From now on, F always represents the three dressing functions. If an equations contains F, one have to keep in mind that $F \in \{A, B, C\}$.

less and less reliable. This problem is more severe for lower temperatures since the number of Matsubara frequencies increases for decreasing temperatures.

In principle, this problem can be resolved if we choose a Matsubara frequency dependent step size for the difference quotient. However, we decided to derive an equation for the derivatives of the dressing functions which can be solved to any desired accuracy. The starting point is the qDSE in the chiral limit. In terms of the dressing functions, it is given by

$$C(\omega_n, x) = Z_2 + \frac{8}{3}\frac{T}{\widetilde{\omega}_n} \sum_l \iint\limits_{y,z} \frac{\alpha_{\text{eff}}(s)}{s} \frac{N_C}{D} \,, \tag{4.24a}$$

$$A(\omega_n, x) = Z_2 + \frac{8}{3}\frac{T}{x} \sum_l \iint\limits_{y,z} \frac{\alpha_{\text{eff}}(s)}{s} \frac{N_A}{D} \,, \tag{4.24b}$$

$$B(\omega_n, x) = 4T \sum_l \iint\limits_{y,z} \frac{\alpha_{\text{eff}}(s)}{s} \frac{N_B}{D} \,. \tag{4.24c}$$

For the sake of brevity, we use the abbreviation

$$\sum_l \iint\limits_{y,z} := \sum_{l=-N_\omega-1}^{N_\omega} \int_{\varepsilon^2}^{\Lambda^2-\omega_l^2} \mathrm{d}y \, \sqrt{y} \int_{-1}^{1} \mathrm{d}z \tag{4.25}$$

for the Matsubara sum and the integrals. Furthermore, we define

$$D := \widetilde{\omega}_l^2 C^2 + yA^2 + B^2 \,, \tag{4.26a}$$

$$N_F := \left(f_1^F \widetilde{\omega}_l C + f_2^F A \right) (1 - \delta_{BF}) + \delta_{BF} B \,, \tag{4.26b}$$

where

$$f_1^C := \frac{1}{2} + \frac{\Omega_{nl}^2}{s} \,, \tag{4.27a}$$

$$f_2^C := \left(\sqrt{xy}\, z - y \right) \frac{\Omega_{nl}}{s} \,, \tag{4.27b}$$

$$f_1^A := \left(x - \sqrt{xy}\, z \right) \frac{\Omega_{nl}}{s} \,, \tag{4.27c}$$

$$f_2^A := \left[\left(1 - \frac{\Omega_{nl}^2}{s} \right) \frac{\left(\sqrt{x}\, z - \sqrt{y} \right) \left(\sqrt{x} - \sqrt{y}\, z \right)}{s - \Omega_{nl}^2} + \frac{1}{2} z \right] \sqrt{xy} \,. \tag{4.27d}$$

Note that we omitted the (ω_l, y)-dependence of C, A, and B in (4.26a) and (4.26b) as well as any dependence on external quantities (ω_n and x) in $f_{1,2}^F$.

The equations determining the μ-derivatives of the dressing functions are now obtained by applying $\partial/\partial\mu$ to the qDSE. Thus, the coupled equations for the first derivative of the dressing functions with respect to the chemical potential read

$$\frac{\partial C(\omega_n, x)}{\partial \mu} = \frac{1}{\widetilde{\omega}_n}\left(-\mathrm{i}\Sigma_C(\omega_n, x) + \frac{8}{3}T\sum_l \iint\limits_{y,z} K_1^C\right), \tag{4.28a}$$

$$\frac{\partial A(\omega_n, x)}{\partial \mu} = \frac{8}{3}\frac{T}{x}\sum_l \iint\limits_{y,z} K_1^A\,, \tag{4.28b}$$

$$\frac{\partial B(\omega_n, x)}{\partial \mu} = 4T\sum_l \iint\limits_{y,z} K_1^B\,, \tag{4.28c}$$

where the integral kernels are given by

$$\begin{aligned} K_1^F &:= \frac{\alpha_{\mathrm{eff}}(s)}{s}\frac{\partial}{\partial\mu}\frac{N_F}{D} \\ &= \frac{\alpha_{\mathrm{eff}}(s)}{s}\frac{1}{D}\left(-\frac{N_F}{D}\frac{\partial D}{\partial\mu} + \frac{\partial N_F}{\partial\mu}\right). \end{aligned} \tag{4.29}$$

With the numerator and denominator functions defined in (4.26a) and (4.26b), their derivatives are straightforward and given by

$$\frac{\partial D}{\partial\mu} = 2\left[\left(\mathrm{i}C + \widetilde{\omega}_l\frac{\partial C}{\partial\mu}\right) + yA\frac{\partial A}{\partial\mu} + B\frac{\partial B}{\partial\mu}\right] \tag{4.30}$$

and

$$\frac{\partial N_F}{\partial\mu} = \left[f_1^F\left(\mathrm{i}C + \widetilde{\omega}_l\frac{\partial C}{\partial\mu}\right) + f_2^F\frac{\partial A}{\partial\mu}\right](1-\delta_{BF}) + \delta_{BF}\frac{\partial B}{\partial\mu}\,. \tag{4.31}$$

Since our aim is the calculation of the quark pressure's Taylor coefficients with respect to μ about $\mu = 0$, we actually need the μ-derivatives of the dressing functions evaluated at vanishing chemical potential only. According to (4.22), we define

$$\begin{aligned} \left.\frac{\partial F(\omega_n, x)}{\partial\mu}\right|_{\mu=0} &= \mathrm{i}\left.\frac{\partial\,\mathrm{Im}(F(\omega_n, x))}{\partial\mu}\right|_{\mu=0} \\ &=: \mathrm{i}F'(\omega_n, x)\,. \end{aligned} \tag{4.32}$$

With

$$\begin{aligned} \left.\frac{\partial D}{\partial\mu}\right|_{\mu=0} &= 2\mathrm{i}\left[\left(C + \omega_l C'\right)\omega_l C + yAA' + BB'\right] \\ &=: \mathrm{i}D' \end{aligned} \tag{4.33}$$

and

$$\begin{aligned}\left.\frac{\partial N_F}{\partial\mu}\right|_{\mu=0} &= \mathrm{i}\left\{\left[f_1^F\left(C+\omega_l\,C'\right)+f_2^F\,A'\right](1-\delta_{BF})+\delta_{BF}\,B'\right\}\\ &=: \mathrm{i}\,N_F'\ ,\end{aligned} \tag{4.34}$$

we can write the integral kernel at vanishing chemical potential as

$$K_1^F\big|_{\mu=0} = \mathrm{i}\,\frac{\alpha_{\mathrm{eff}}(s)}{s}\,\frac{1}{D}\left(N_F' - \frac{N_F\,D'}{D}\right)\ . \tag{4.35}$$

Finally, the equations for the first μ-derivative become

$$C'(\omega_n,x) = -\frac{1}{\omega_n}\left(\Sigma_C(\omega_n,x)+\frac{8}{3}T\sum_l\iint\limits_{y,z}\mathrm{i}K_1^C\big|_{\mu=0}\right)\ , \tag{4.36a}$$

$$A'(\omega_n,x) = -\frac{8}{3}\frac{T}{x}\sum_l\iint\limits_{y,z}\mathrm{i}K_1^A\big|_{\mu=0}\ , \tag{4.36b}$$

$$B'(\omega_n,x) = -4T\sum_l\iint\limits_{y,z}\mathrm{i}K_1^B\big|_{\mu=0}\ . \tag{4.36c}$$

As the qDSE itself, the equations (4.36a), (4.36b), and (4.36c) determining C', A', and B' are self-consistent. Equations for the higher derivatives are obtained by further derivatives of the qDSE with respect to μ. For example, with

$$\begin{aligned}\left.\frac{\partial^2 F(\omega_n,x)}{\partial\mu^2}\right|_{\mu=0} &= \left.\frac{\partial^2\,\mathrm{Re}(F(\omega_n,x))}{\partial\mu^2}\right|_{\mu=0}\\ &=: F''(\omega_n,x)\end{aligned} \tag{4.37}$$

we find

$$C''(\omega_n,x) = \frac{2}{\omega_n}\left(C'(\omega_n,x)+\frac{4}{3}T\sum_l\iint\limits_{y,z}K_2^C\big|_{\mu=0}\right)\ , \tag{4.38a}$$

$$A''(\omega_n,x) = \frac{8}{3}\frac{T}{x}\sum_l\iint\limits_{y,z}K_2^A\big|_{\mu=0}\ , \tag{4.38b}$$

$$B''(\omega_n,x) = 4T\sum_l\iint\limits_{y,z}K_2^B\big|_{\mu=0}\ , \tag{4.38c}$$

where the kernel is given by

$$K_2^F := \frac{\alpha_{\mathrm{eff}}(s)}{s}\,\frac{\partial^2}{\partial\mu^2}\,\frac{N_F}{D}\ . \tag{4.39}$$

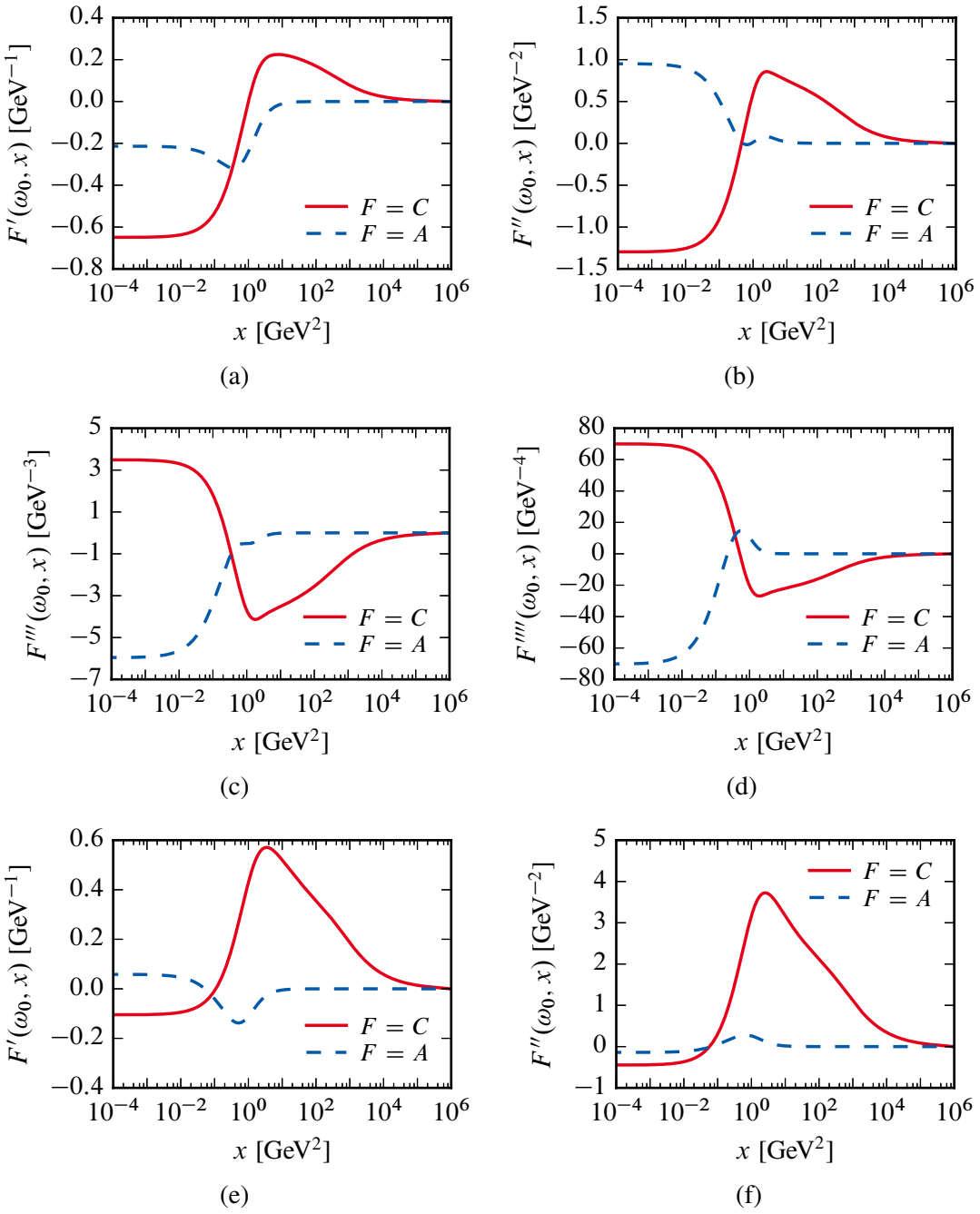

Figure 4.2.: μ-derivatives of the dressing functions C and A for the zeroth Matsubara frequency at $T = 1.5\,T_c$ ((a) to (d)) and $T = 0.8\,T_c$ ((e) and (f)).

We computed the first, second, third, and fourth derivative of the dressing functions with respect to μ at $\mu = 0$. Since the equations for the derivatives inherit the self-consistent nature of the qDSE, we discretise the derivatives on a momentum grid and solve the equations with the same fixed-point iteration method we use to solve the DSE for the quark propagator. Since the first derivative needs the original dressing functions as input, the momentum grid for the derivatives is the same as for the qDSE. The initial value for all derivatives, ignoring their different momentum dimensions for the moment, is 0.25 at each grid point. We checked the dependence of the obtained solutions on the initial value by increasing and decreasing it by an order of magnitude. Despite the different inital values, the iteration always converged to the same solution.

In Figure 4.2 we present exemplarily the first four derivatives of the dressing functions C and A at a temperature of $T = 1.5\,T_\mathrm{c}$ and $T = 0.8\,T_\mathrm{c}$. The derivatives of A are nonzero in the IR and drop to zero for squared momenta $x \gtrsim 80\,\mathrm{GeV}^2$. This is consistent with the fact that the medium dominantly affects the infrared and furthermore with our solutions of the qDSE. Consequently, the spurious behaviour of $\mathrm{Im}(C)$ at nonzero chemical potential (see Section 3.2.4) is visible in the μ-derivatives of C. They acquire nonzero values almost over the entire momentum domain and drop to zero only in deep UV close to the cutoff. This holds also below the critical temperature. Furthermore, at temperatures below T_c, we observe that the shape of the derivatives of C stays the same.

4.3. Taylor Coefficients

Up to this point, we solved the qDSE in the medium as well as the equations determining the derivatives of the dressing functions with respect to μ. Thus, we are now prepared to compute the Taylor coefficients of the quark pressure according to (4.5). Since the dressing functions and their derivatives are known only on a finite momentum grid with IR cutoff ε and UV cutoff $\Lambda^2 - \omega_l^2$ (cf. Eq. (3.44)), we write the quark pressure (4.20) as

$$\wp(T,\mu) = \frac{3T}{2\pi^2} \sum_{l=-N_\omega-1}^{N_\omega} \int_{\varepsilon^2}^{\Lambda^2-\omega_l^2} \mathrm{d}y\, \sqrt{y} \left(\mathrm{Tr}\log\frac{S^{-1}}{T} - \frac{1}{2}\,\mathrm{Tr}\big[\mathbb{1} - S_0^{-1}S\big] \right) , \tag{4.40}$$

where we used spherical coordinates with $y = \boldsymbol{q}^2$ and integrated out the trivial angular integrals. Furthermore, we omitted the dependencies of the integrand for the sake of brevity. This equation is the starting point for the calculation of the Taylor coefficients.

Before we proceed, we would like to mention an important fact regarding the pressure and its Taylor coefficients with respect to μ about $\mu = 0$. As the grand canonical potential $\Omega(T,\mu)$ is invariant under charge conjugation only the even coefficients $d_{2k}(T)$, $k \in \mathbb{N}$, are nonzero. Thus, the odd coefficients serve as a check for our numerics since they must vanish for all temperatures. Furthermore, in the limit $T \to \infty$, the reduced pressure approaches the Stefan-Boltzmann (SB)

limit (for $N_\mathrm{f} = 2$ massless flavours with the same chemical potential) [80]

$$\bar{\wp}(T,\mu) \xrightarrow{T\to\infty} \bar{\wp}_\mathrm{SB}(T,\mu) := \frac{37\pi^2}{90} + \left(\frac{\mu}{T}\right)^2 + \frac{1}{2\pi^2}\left(\frac{\mu}{T}\right)^4 \tag{4.41}$$

with the only non-vanishing Taylor coefficients

$$c_2^\mathrm{SB} = 1\,, \qquad c_4^\mathrm{SB} = \frac{1}{2\pi^2} \approx 0.05\,. \tag{4.42}$$

Thus, it can be checked if c_2 and c_4 approach the SB limit for high temperatures.

Coefficient d_1

The first coefficient is simply the first derivative of the pressure with respect to μ, viz.

$$\begin{aligned} d_1(T) &= \left.\frac{\partial\wp(T,\mu)}{\partial\mu}\right|_{\mu=0} \\ &= \frac{3T}{2\pi^2} \sum_{l=-N_\omega-1}^{N_\omega} \int_{\varepsilon^2}^{\Lambda^2-\omega_l^2} \mathrm{d}y\,\sqrt{y}\left(\frac{\partial}{\partial\mu}\,\mathrm{Tr}\log\frac{S^{-1}}{T} + \frac{1}{2}\frac{\partial}{\partial\mu}\,\mathrm{Tr}\big[S_0^{-1}S\big]\right)\Bigg|_{\mu=0} \end{aligned} \tag{4.43}$$

Using the chain rule, the first part of the integrand reads

$$\begin{aligned} \frac{\partial}{\partial\mu}\,\mathrm{Tr}\log\frac{S^{-1}}{T} &= \mathrm{Tr}\left[S\,\frac{\partial S^{-1}}{\partial\mu}\right] \\ &= \frac{1}{D}\,\mathrm{Tr}\left[\left(\mathrm{i}\widetilde{\omega}_l\,\gamma_4 C + \mathrm{i}\not{q}A + B\right)\left(-\mathrm{i}\gamma_4\left(\mathrm{i}C + \widetilde{\omega}_l\,\frac{\partial C}{\partial\mu}\right) - \mathrm{i}\not{q}\,\frac{\partial A}{\partial\mu} + \frac{\partial B}{\partial\mu}\right)\right], \end{aligned} \tag{4.44}$$

where D is defined in Eq. (4.26a). After the matrix products are carried out (in Dirac space), we are left with terms proportional to $\mathbb{1}$, γ_4, $\not{q}$, and $\gamma_4\not{q}$. However, only the trace over the former yields a nonzero value, $\mathrm{Tr}\,\mathbb{1} = 4$, and the Dirac trace over the rest vanishes. Thus,

$$\begin{aligned} \frac{\partial}{\partial\mu}\,\mathrm{Tr}\log\frac{S^{-1}}{T} &= \frac{4}{D}\left[\left(\mathrm{i}C + \widetilde{\omega}_l\,\frac{\partial C}{\partial\mu}\right)\widetilde{\omega}_l\,C + yA\,\frac{\partial A}{\partial\mu} + B\,\frac{\partial B}{\partial\mu}\right] \\ &= \frac{2}{D}\,\frac{\partial D}{\partial\mu}\,. \end{aligned} \tag{4.45}$$

Similarly, we find

$$\frac{\partial}{\partial\mu}\,\mathrm{Tr}\big[S_0^{-1}S\big] = \frac{2Z_2}{D}\left[-\frac{1}{D}\,\frac{\partial D}{\partial\mu}\left(\widetilde{\omega}_l^2\,C + yA\right) + \left(2\mathrm{i}C + \widetilde{\omega}_l\,\frac{\partial C}{\partial\mu}\right)\widetilde{\omega}_l + y\,\frac{\partial A}{\partial\mu}\right]. \tag{4.46}$$

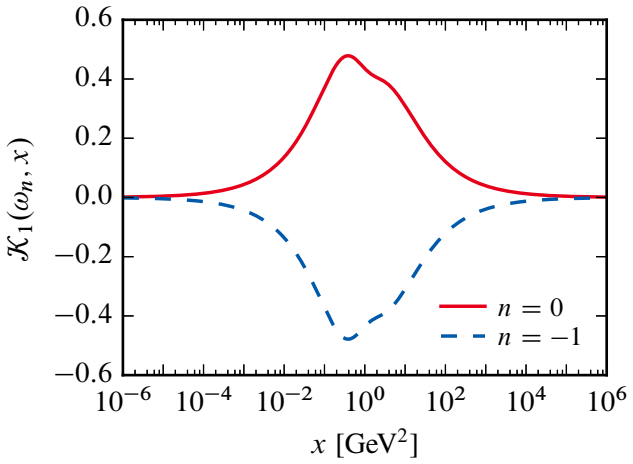

Figure 4.3.: Integral kernel of the first Taylor coefficient (cf. Eq. (4.50)) at $T = 1.5\,T_\mathrm{c}$.

With the definition

$$\mathcal{N} := \tilde{\omega}_l^2\, C + yA\,, \tag{4.47}$$

the first Taylor coefficient reads

$$d_1(T) = \frac{3T}{\pi^2} \sum_{l=-N_\omega-1}^{N_\omega} \int_{\varepsilon^2}^{\Lambda^2-\omega_l^2} \mathrm{d}y\, \frac{\sqrt{y}}{D} \left[\frac{\partial D}{\partial \mu} \left(1 - \frac{Z_2\,\mathcal{N}}{D} \right) + Z_2 \frac{\partial \mathcal{N}}{\partial \mu} \right] \Bigg|_{\mu=0} . \tag{4.48}$$

Finally, using Eq. (4.33) and

$$\begin{aligned} \frac{\partial \mathcal{N}}{\partial \mu}\bigg|_{\mu=0} &= \mathrm{i} \Big[\left(2C + \omega_l\, C' \right) \omega_l + yA' \Big] \\ &=: \mathrm{i}\,\mathcal{N}' \end{aligned} \tag{4.49}$$

we arrive at

$$d_1(T) = \mathrm{i}\, \frac{3T}{\pi^2} \sum_{l=-N_\omega-1}^{N_\omega} \int_{\varepsilon^2}^{\Lambda^2-\omega_l^2} \mathrm{d}y\, \underbrace{\frac{\sqrt{y}}{D} \left[D' \left(1 - \frac{Z_2\,\mathcal{N}}{D} \right) + Z_2\,\mathcal{N}' \right]}_{=:\mathcal{K}_1} . \tag{4.50}$$

Since $d_1(T)$ is the derivative of the pressure with respect to the chemical potential, it is physically interpreted as the quark density and should therefore vanish at $\mu = 0$. This would be consistent with the fact that only even coefficients are nonzero. First of all, we observe that $d_1(T)$ is purely imaginary, which is already a strong evidence that it must vanish since the pressure is a real-valued quantity. Furthermore, we can exploit the symmetries

$$F(\omega_n, x; \mu = 0) = F(\omega_{-n-1}, x; \mu = 0) \tag{4.51}$$

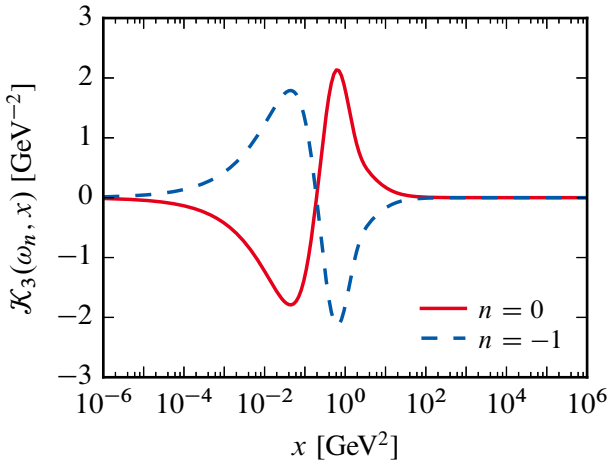

Figure 4.4.: Integral kernel of the third Taylor coefficient (cf. Eq. (4.55)) at $T = 1.5\,T_\mathrm{c}$.

and

$$F'(\omega_n, x) = -F'(\omega_{-n-1}, x)\ . \tag{4.52}$$

For example, $D = \omega_l^2 C^2 + yA^2 + B^2$ is symmetric with respect to the Matsubara sum since the dressing functions itself are symmetric and the antisymmetric Matsubara frequency appears squared. On the other hand,

$$D' = 2\Big[\big(C + \omega_l C'\big)\,\omega_l\, C + yAA' + BB'\Big] \tag{4.53}$$

is antisymmetric with respect to the Matsubara sum since every symmetric quantity is multiplied by an antisymmetric one. Altogether, the kernel $\mathcal{K}_1$ is an antisymmetric quantity with respect to the Matsubara sum and hence vanishes. In Figure 4.3, we present the kernel for the Matsubara sum pairs $n = 0$ and $n = -1$ at $T = 1.5\,T_\mathrm{c}$. As expected, $\mathcal{K}_1(\omega_0, x) = -\mathcal{K}_1(\omega_{-1}, x)$. Note that this discussion regarding the symmetry with respect to the Matsubara sum is independent of the temperature. Thus, $d_1(T) = 0$ for all temperatures T.

Coefficient d_3

Analogous to the first coefficient, the third one must vanish as well. The calculation of three derivatives of the pressure with respect to μ is straightforward but lengthy. Thus, we give only the final result which reads

$$d_3(T) = \mathrm{i}\,\frac{T}{2\pi^2} \sum_{l=-N_\omega-1}^{N_\omega} \int_{\varepsilon^2}^{\Lambda^2-\omega_l^2} \mathrm{d}y\ \mathcal{K}_3(\omega_l, y)\ , \tag{4.54}$$

where the integral kernel is given by

$$\begin{aligned}\mathcal{K}_3(\omega_l, y) := \frac{\sqrt{y}}{D^4}\Big\{ & 6 Z_2 \mathcal{N} D'^3 + 2 D D' \left[-D'^2 - 3 Z_2 \left(D' \mathcal{N}' - N D''\right)\right] \\ & - D^2 \left[3 D' \left(D'' + Z_2 \mathcal{N}''\right) + Z_2 \left(3 \mathcal{N}' D'' + \mathcal{N} D'''\right)\right] \\ & + D^3 \left(D''' + Z_2 \mathcal{N}'''\right)\Big\}\end{aligned} \tag{4.55}$$

with

$$D'' := \left.\frac{\partial^2 D}{\partial \mu^2}\right|_{\mu=0}, \qquad D''' := -\mathrm{i} \left.\frac{\partial^3 D}{\partial \mu^3}\right|_{\mu=0}, \tag{4.56}$$

$$\mathcal{N}'' := \left.\frac{\partial^2 \mathcal{N}}{\partial \mu^2}\right|_{\mu=0}, \qquad \mathcal{N}''' := -\mathrm{i} \left.\frac{\partial^3 \mathcal{N}}{\partial \mu^3}\right|_{\mu=0}. \tag{4.57}$$

Like the first Taylor coefficient, $d_3(T)$ is purely imaginary. The analysis regarding the Matsubara sum symmetry yields that the kernel is, as expected, antisymmetric. This can also be seen from Figure 4.4, where we show the kernel $\mathcal{K}_3$ for the two Matsubara sum pairs $n = 0$ and $n = -1$ at $T = 1.5 T_\mathrm{c}$. Consequently, $d_3(T) = 0$ for all T.

Coefficient d_2

The second Taylor coefficient is the first nonvanishing one (apart from the pressure itself, which is the zeroth coefficient). Being the second derivative of the quark pressure, it can be physically interpreted as the quark number susceptibility at $\mu = 0$. It is given by

$$d_2(T) = \frac{3T}{2\pi^2} \sum_{l=-N_\omega-1}^{N_\omega} \int_{\varepsilon^2}^{\Lambda^2-\omega_l^2} \mathrm{d}y \; \mathcal{K}_2(\omega_l, y) \tag{4.58}$$

with the kernel

$$\mathcal{K}_2(\omega_l, y) := \frac{\sqrt{y}}{D}\left[\left(1 - \frac{Z_2 \mathcal{N}}{D}\right)\left(D'' + \frac{D'^2}{D}\right) + Z_2 \left(\mathcal{N}'' + \frac{2 D' \mathcal{N}}{D} - \frac{\mathcal{N} D'^2}{D^2}\right)\right]. \tag{4.59}$$

The coefficient does not vanish due to the Matsubara sum, because the kernel is now symmetric with respect to the summation. However, in the course of calculating d_2 we observed that it is not convergent. A possible reason is that the integral kernel does not fall off quickly enough for large momenta. In Figure 4.5, we present the kernel for the zeroth Matsubara frequency at $T = 1.5 T_\mathrm{c}$. Indeed, the large-x behaviour is such that the kernel does not drop to zero in the UV. For example, it acquires a value of $-2 \times 10^{-3}\,\mathrm{GeV}^{-1}$ at the cutoff.

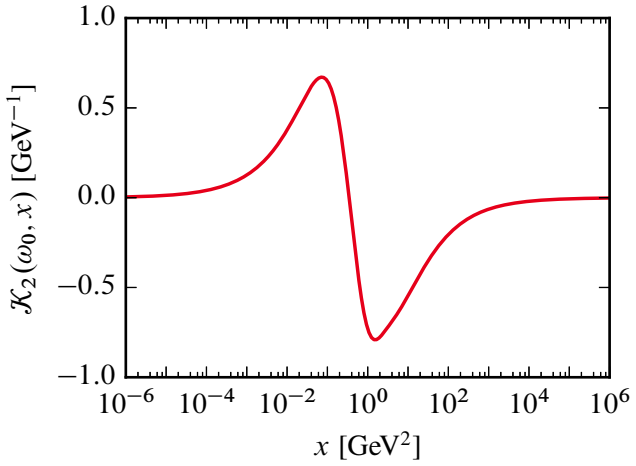

Figure 4.5.: Integral kernel of the second Taylor coefficient at $T = 1.5\,T_c$.

Λ/Λ'	4/3	1/2	1/3	1/4
$d_2^{\Lambda}/d_2^{\Lambda'}$	1.340	0.496	0.330	0.247

Table 4.1.: Ratios of d_2 obtained from calculations with different UV cutoffs.

In order to investigate the nature of the divergence, we calculated the ratio $d_2^{\Lambda}/d_2^{\Lambda'}$ where d_2^{Λ} and $d_2^{\Lambda'}$ indicates a calculation of the second Taylor coefficient with different cutoffs Λ and Λ', respectively. The results are shown in Table 4.1, where we fixed $\Lambda = 1\,\text{TeV}$ and varied Λ'. Apparently, the second Taylor coefficient scales within the numerical accuarcy linearly with the cutoff, indicating that it suffers from a linear divergence.

Unfortunately, we have not resolved this issue yet and one has to implement a suitable subtraction method to cancel the linear divergence without changing the physics.

5. Summary and Outlook

In this thesis we have studied the Taylor coefficients of the quark pressure with respect to μ about $\mu = 0$ from a Dyson–Schwinger perspective. As a starting point, we derived the DSE for the dressed quark propagator. This equation is first solved in the vacuum and subsequently at nonzero temperature and density. Since the qDSE is coupled to higher correlation functions, we employed a rainbow-ladder truncation to obtain a closed system of equations which is then solved numerically. We can confirm the spurious behaviour of the temporal dressing function at nonzero chemical potential, namely that it shows an unphysical enhancement in the ultraviolet. This was also found in a recent work, see Ref. [75]. Since the Taylor coefficients contain μ-derivatives of the quark propagator, we derived exact and self-consistent equations determining these derivatives. The reason is our observance that a simple difference quotient lacks the required accuracy. We solved these derivative equations up to the fourth derivative. Finally, we investigated the first, second, and third Taylor coefficients d_1, d_2, and d_3. We found that d_1 and d_3 vanish for all temperatures which is in accordance with the fact that only the even coefficients of the quark pressure are nonzero. Unfortunately, we found that the second coefficient suffers from a linear divergence and we have not resolved this problem yet.

The next and most urgent step is to investigate the divergence of the second coefficient in detail. It is still unclear where the divergence exactly comes from and how to define a proper subtraction method to remove the linear divergence. Furthermore, it is desirable to obtain higher coefficients like the fourth and the sixth since we expect that these quantities are convergent.

A. Notation and Conventions

A.1. Units

Throughout this thesis we use natural units, i.e.

$$\hbar = c = k_{\mathrm{B}} = 1 \,. \tag{A.1}$$

Thus, the only remaining unit is the energy (given in electron volts, eV). For example, the SI-units metre (m) for length and kelvin (K) for temperature are related to the energy via

$$1\,\mathrm{m} \approx 5.1 \times 10^{6}\,\mathrm{eV}^{-1} \,, \qquad 1\,\mathrm{K} \approx 8.6 \times 10^{-5}\,\mathrm{eV} \,. \tag{A.2}$$

A.2. Euclidean Space-Time

We work solely in four-dimensional Euclidean space-time, i.e. the metric tensor is given by

$$g_{\mu\nu} := \begin{bmatrix} 1 & 0 & 0 & 0 \\ 0 & 1 & 0 & 0 \\ 0 & 0 & 1 & 0 \\ 0 & 0 & 0 & 1 \end{bmatrix} . \tag{A.3}$$

Thus, it is not necessary to distinguish between co- and contravariant indices and the scalar product of two four-vectors $x = (x_4, \boldsymbol{x})$ and $y = (y_4, \boldsymbol{y})$ is given by $x \cdot y = g_{\mu\nu} x_\mu y_\nu = x_4 y_4 + \boldsymbol{x} \cdot \boldsymbol{y}$. We emphasise the Euclidean space-time by using the index "4" for the first component of a four-vector. As usual, bold-face letters denote three-vectors. Consequently, the Dirac algebra is defined through

$$\{\gamma_\mu, \gamma_\nu\} := \gamma_\mu \gamma_\nu + \gamma_\nu \gamma_\mu = 2\delta_{\mu\nu} \mathbb{1}_{4\times4} \,, \tag{A.4}$$

where $\mathbb{1}_{4\times4}$ denotes the 4×4 identity matrix. Relation (A.4) can be realised by choosing the Dirac representation

$$\gamma_4 = \begin{bmatrix} \mathbb{1}_{2\times2} & 0 \\ 0 & -\mathbb{1}_{2\times2} \end{bmatrix} , \qquad \gamma_i = \begin{bmatrix} 0 & -\mathrm{i}\sigma_i \\ \mathrm{i}\sigma_i & 0 \end{bmatrix} \tag{A.5}$$

with the Pauli matrices

$$\sigma_1 = \mathbb{1}_{2\times2} \,, \qquad \sigma_2 = \begin{bmatrix} 0 & -\mathrm{i} \\ \mathrm{i} & 0 \end{bmatrix} , \qquad \sigma_3 = \begin{bmatrix} 1 & 0 \\ 0 & -1 \end{bmatrix} . \tag{A.6}$$

This choice for the gamma matrices implies that they are Hermitian, i.e. $\gamma_\mu^\dagger = \gamma_\mu$. Furthermore, the fifth gamma matrix is defined by

$$\gamma_5 := \gamma_4 \gamma_1 \gamma_2 \gamma_3 = \begin{bmatrix} 0 & \mathbb{1}_{2\times 2} \\ \mathbb{1}_{2\times 2} & 0 \end{bmatrix} \tag{A.7}$$

and has the properties

$$\gamma_5^2 = \mathbb{1}_{4\times 4} \,, \qquad \gamma_5^\dagger = \gamma_5 \,, \qquad \{\gamma_\mu, \gamma_5\} = 0 \,. \tag{A.8}$$

The contraction of a quantity with the gamma matrices is abbreviated using the Feynman slash notation, i.e. $\not{a}$ is to be understood as $\gamma_\mu a_\mu$. Using the definition of the Dirac algebra (A.4), it is straightforward to obtain the identities

$$\begin{aligned} \gamma_\mu \gamma_\mu &= 4\mathbb{1}_{4\times 4} \,, \qquad \not{a}\not{a} = a^2 \mathbb{1}_{4\times 4} \,, \\ \gamma_\mu \not{a} \gamma_\mu &= -2\not{a} \,, \qquad \not{a}\not{b}\not{a} = 2(a\cdot b)\not{a} - a^2 \not{b} \,. \end{aligned} \tag{A.9}$$

Finally, as already employed in the above formulas, we make use of the Einstein summation convention: There is an implicit sum with appropriate limits over repeated free indices. For example, $\gamma_\mu \gamma_\mu \equiv \sum_{\mu=1}^{4} \gamma_\mu \gamma_\mu$.

A.3. Fourier Transform

We use the following conventions for the Fourier transform:

$$f(p) = \int \mathrm{d}^4 x \, f(x) \, \mathrm{e}^{-\mathrm{i} p\cdot x} \,, \tag{A.10a}$$

$$f(p,q) = \int \mathrm{d}^4 x \int \mathrm{d}^4 y \, f(x,y) \, \mathrm{e}^{-\mathrm{i}(p\cdot x - q\cdot y)} \,, \tag{A.10b}$$

while the inverse Fourier transform is given by

$$f(x) = \int \frac{\mathrm{d}^4 p}{(2\pi)^4} \, f(p) \, \mathrm{e}^{\mathrm{i} p\cdot x} \,, \tag{A.11a}$$

$$f(x,y) = \int \frac{\mathrm{d}^4 p}{(2\pi)^4} \int \frac{\mathrm{d}^4 q}{(2\pi)^4} \, f(p,q) \, \mathrm{e}^{\mathrm{i}(p\cdot x - q\cdot y)} \,. \tag{A.11b}$$

It shall be emphasised that we distinguish between a function and its Fourier transform solely by the appearing argument rather than introducing a special notation.

These conventions imply for the delta function that

$$(2\pi)^4 \delta^{(4)}(p) = \int \mathrm{d}^4 x \, \mathrm{e}^{-\mathrm{i} p\cdot x} \,. \tag{A.12}$$

A.4. Functional Derivative

In general, a functional is a linear map from a vector space into the underlying field. This vector space is commonly a normed space of functions over the real or complex numbers, which will be considered here (i.e. the functional takes a function as its argument and yields a number). For the sake of simplicity, we shall consider here real-valued functions which depend only on one variable. The generalisation to higher dimensions is straightforward.

The functional derivative of a functional $F[f]$ is defined by the difference quotient [81]

$$\frac{\delta F[f]}{\delta f(y)} := \lim_{\varepsilon \to 0} \frac{F[f + \varepsilon \delta(x-y)] - F[f]}{\varepsilon} \,, \tag{A.13}$$

where the x-dependence on the right hand side is only formal (x is a "silent argument" like the argument of the function f). [1]

The above definition leads to the elementary functional derivative

$$\frac{\delta f(x)}{\delta f(y)} = \delta(x-y) \,, \tag{A.14}$$

which is the continuum version of $\partial x_i / \partial x_j = \delta_{ij}$. Note that additional Kronecker deltas appear in (A.14) if the function carries additional degrees of freedom. For example, let f_a be a function with an additional degree of freedom denoted by a (e.g. a Dirac index). Its functional derivative then extends to

$$\frac{\delta f_a(x)}{\delta f_b(y)} = \delta_{ab}\, \delta(x-y) \,. \tag{A.15}$$

[1] From a more rigorous point of view, definition (A.13) is a bit problematic since the delta function exists only in the distributional sense and the addition $f + \varepsilon\delta$ is not defined. A more unambiguous definition is

$$\frac{\delta F[f]}{\delta f(y)} = \lim_{\sigma \to 0} \lim_{\varepsilon \to 0} \frac{F[f + \varepsilon \delta_\sigma(x-y)] - F[f]}{\varepsilon} \,,$$

where δ_σ is a smooth function which satisfies $\lim_{\sigma\to 0} \delta_\sigma(x-y) = \delta(x-y)$.

B. Path Integral of a Total Derivative

In the following we prove the identity (2.42), which is the starting point of the derivative of the DSEs. For simplicity, we consider a Euclidean real scalar theory with the partition function

$$\mathcal{Z}[J] := \int \mathcal{D}\varphi \exp\left\{-I[\varphi] + \int \mathrm{d}^4x\, J(x)\varphi(x)\right\} \tag{B.1}$$

and we have to show

$$0 = \int \mathcal{D}\varphi \frac{\delta}{\delta\varphi(y)} \exp\left\{-I[\varphi] + \int \mathrm{d}^4x\, J(x)\varphi(x)\right\} . \tag{B.2}$$

Besides the usual assumption that the path integral is well defined, we assume that the measure is invariant under the transformation $\varphi \to \varphi + \varepsilon f$ with an infinitesimal $\varepsilon > 0$ and an arbitrary function f. It follows that

$$\mathcal{Z}[J] = \int \mathcal{D}\varphi \underbrace{\exp\left\{-I[\varphi + \varepsilon f] + \int \mathrm{d}^4x\, J(x)\big(\varphi(x) + \varepsilon f(x)\big)\right\}}_{=:\mathcal{J}} . \tag{B.3}$$

An expansion with respect to ε of the exponential on the right hand side of (B.3) yields

$$\begin{aligned}\mathcal{J} = {} & \exp\left\{-I[\varphi] + \int \mathrm{d}^4x\, J(x)\varphi(x)\right\} \\ & + \varepsilon \int \mathrm{d}^4y\, f(y) \left(-\frac{\delta I[\varphi]}{\delta\varphi(y)} + J(y)\right) \exp\left\{-I[\varphi] + \int \mathrm{d}^4x\, J(x)\varphi(x)\right\} \\ & + \mathcal{O}(\varepsilon^2) .\end{aligned} \tag{B.4}$$

Thus, Eq. (B.3) can be written as

$$0 = \int \mathrm{d}^4y\, f(y) \int \mathcal{D}\varphi \left(-\frac{\delta I[\varphi]}{\delta\varphi(y)} + J(y)\right) \exp\left\{-I[\varphi] + \int \mathrm{d}^4x\, J(x)\varphi(x)\right\} + \mathcal{O}(\varepsilon) . \tag{B.5}$$

Since f was arbitrary and ε infinitesimal, we have

$$\begin{aligned} 0 &\stackrel{!}{=} \int \mathcal{D}\varphi \left(-\frac{\delta I[\varphi]}{\delta\varphi(y)} + J(y)\right) \exp\left\{-I[\varphi] + \int \mathrm{d}^4x\, J(x)\varphi(x)\right\} \\ &= \int \mathcal{D}\varphi \frac{\delta}{\delta\varphi(y)} \exp\left\{-I[\varphi] + \int \mathrm{d}^4x\, J(x)\varphi(x)\right\} . \end{aligned} \tag{B.6}$$

Bibliography

[1] M. Gell-Mann, "A schematic model of baryons and mesons", *Physics Letters*, vol. 8, p. 214, 1964.

[2] G. Zweig, *An SU_3 model for strong interaction symmetry and its breaking II*, CERN report no. 8419/TH.412, 1964.

[3] E. D. Bloom et al., "High-Energy Inelastic $e - p$ Scattering at 6° and 10°", *Physical Review Letters*, vol. 23, p. 930, 1969.

[4] M. Breidenbach et al., "Observed Behavior of Highly Inelastic Electron-Proton Scattering", *Physical Review Letters*, vol. 23, p. 935, 1969.

[5] H. Fritzsch, M. Gell-Mann, and H. Leutwyler, "Advantages of the color octet gluon picture", *Physics Letters B*, vol. 47, p. 365, 1973.

[6] S. Weinberg, "Non-Abelian Gauge Theories of the Strong Interaction", *Physical Review Letters*, vol. 31, p. 494, 1973.

[7] D. J. Gross and F. Wilczek, "Ultraviolet Behavior of Non-Abelian Gauge Theories", *Physical Review Letters*, vol. 30, p. 1343, 1973.

[8] H. D. Politzer, "Reliable Perturbative Results for Strong Interactions?", *Physical Review Letters*, vol. 30, p. 1346, 1973.

[9] S. Bethke, "Experimental tests of asymptotic freedom", *Progress in Particle and Nuclear Physics*, vol. 58, p. 351, 2007, `arXiv:hep-ex/0606035`.

[10] M. Stephanov, "QCD phase diagram: an overview", in proceedings of "XXIV International Symposium on Lattice Field Theory", *PoS(LAT2006)024* (2006), `arXiv:hep-lat/0701002`.

[11] P. Braun-Munzinger and J. Wambach, "Phase diagram of strongly interacting matter", *Review of Modern Physics*, vol. 81, p. 1031, 2009, `arXiv:0801.4256 [hep-ph]`.

[12] J. Letessier and J. Rafelski, *Hadrons and Quark–Gluon Plasma* (Cambridge University Press, 2002).

[13] Y. Nambu and G. Jona-Lasinio, "Dynamical Model of Elementary Particles Based on an Analogy with Superconductivity. I", *Physical Review*, vol. 122, p. 345, 1961.

[14] Y. Nambu and G. Jona-Lasinio, "Dynamical Model of Elementary Particles Based on an Analogy with Superconductivity. II", *Physical Review*, vol. 124, p. 246, 1961.

[15] M. Buballa, "NJL-model analysis of dense quark matter", *Physics Reports*, vol. 407, p. 205, 2005, arXiv:hep-ph/0402234.

[16] M. Buballa and S. Carignano, "Inhomogeneous chiral condensates", *Progress in Particle and Nuclear Physics*, vol. 81, p. 39, 2015, arXiv:1406.1367 [hep-ph].

[17] F. J. Dyson, "The *S* Matrix in Quantum Electrodynamics", *Physical Review*, vol. 75, p. 1736, 1949.

[18] J. S. Schwinger, "On the Green's functions of quantized fields. I", *Proceedings of the National Academy of Sciences*, vol. 37, p. 452, 1951.

[19] J. S. Schwinger, "On the Green's functions of quantized fields. II", *Proceedings of the National Academy of Sciences*, vol. 37, p. 455, 1951.

[20] C. Wetterich, "Exact evolution equation for the effective potential", *Physics Letters B*, vol. 301, p. 90, 1993.

[21] J. Braun, L. M. Haas, F. Marhauser, and J. M. Pawlowski, "Phase Structure of Two-Flavor QCD at Finite Chemical Potential", *Physical Review Letters*, vol. 106, p. 022002–1, 2011, arXiv:0908.0008 [hep-ph].

[22] T. K. Herbst, J. M. Pawlowski, and B. J. Schaefer, "Phase structure and thermodynamics of QCD", *Physical Review D*, vol. 88, p. 014007–1, 2013, arXiv:1302.1426 [hep-ph].

[23] D. Nickel, J. Wambach, and R. Alkofer, "Color superconductivity in the strong-coupling regime of Landau gauge QCD", *Physical Review D*, vol. 73, p. 114028, 2006, arXiv:hep-ph/0603163.

[24] C. S. Fischer and J. Lücker, "Propagators and phase structure of $N_f = 2$ and $N_f = 2 + 1$ QCD", *Physics Letters B*, vol. 718, p. 1036, 2013, arXiv:1206.5191 [hep-ph].

[25] D. Müller, M. Buballa, and J. Wambach, "Dyson–Schwinger study of chiral density waves in QCD", *Physics Letters B*, vol. 727, p. 240, 2013, arXiv:1308.4303 [hep-ph].

[26] D. Müller, M. Buballa, and J. Wambach, "Dyson-Schwinger approach to color superconductivity at finite temperature and density", *The European Physical Journal A*, vol. 49, issue 8, article no. 96, p. 1, 2013, arXiv:1303.2693 [hep-ph].

[27] P. Büscher, "Phase diagram of two-color QCD in a Dyson-Schwinger approach", PhD thesis (Technische Universität Darmstadt, 2014).

[28] F. Gao et al., "Phase diagram and thermal properties of strong-interaction matter", *Physical Review D*, vol. 93, p. 094019–1, 2016, arXiv:1507.00875 [nucl-th].

[29] Z. Fodor and S. D. Katz, "A new method to study lattice QCD at finite temperature and chemical potential", *Physics Letters B*, vol. 534, p. 87, 2002, arXiv:hep-lat/0104001.

[30] D. Sexty, "Simulating full QCD at nonzero density using the complex Langevin equation", *Physics Letters B*, vol. 729, p. 108, 2014, arXiv:1307.7748 [hep-lat].

[31] G. Aarts et al., "QCD at nonzero chemical potential: Recent progress on the lattice", *AIP Conference Proceedings*, vol. 1701, p. 020001, 2016, arXiv:1412.0847 [hep-lat].

[32] C. Itzykson and J.-B. Zuber, *Quantum Field Theory* (McGraw Hill, 1980).

[33] M. E. Peskin and D. V. Schroeder, *An Introduction to Quantum Field Theory* (Westview Press, 1995).

[34] P. Pascual and R. Tarrach, *QCD: Renormalization for the Practitioner* (Springer Berlin Heidelberg, 1984).

[35] J. I. Kapusta and C. Gale, *Finite-Temperature Field Theory: Principles and Applications* (Cambridge University Press, 2006).

[36] C. N. Yang and R. L. Mills, "Conservation of Isotopic Spin and Isotopic Gauge Invariance", *Physical Review*, vol. 96, p. 191, 1954.

[37] L. D. Faddeev and V. N. Popov, "Feynman diagrams for the Yang-Mills field", *Physics Letters B*, vol. 25, p. 29, 1967.

[38] C. Becchi, A. Rouet, and R. Stora, "The abelian Higgs Kibble model, unitarity of the *S*-operator", *Physics Letters B*, vol. 52, p. 344, 1974.

[39] C. Becchi, A. Rouet, and R. Stora, "Renormalization of the abelian Higgs-Kibble model", *Communications in Mathematical Physics*, vol. 42, p. 127, 1975.

[40] C. Becchi, A. Rouet, and R. Stora, "Renormalization of Gauge Theories", *Annals of Physics*, vol. 98, p. 287, 1976.

[41] I. V. Tyutin, *Gauge Invariance in Field Theory and Statistical Physics in Operator Formalism*, preprint no. 39 of the Lebedev Physical Institute of the Russian Academy of Sciences, 1975, arXiv:0812.0580 [hep-th].

[42] M. Z. Iofa and I. V. Tyutin, "Gauge invariance of spontaneously broken non-Abelian theories in the Bogolyubov-Parasyuk-Hepp-Zimmermann method", *Theoretical and Mathematical Physics*, vol. 27, p. 316, 1976.

[43] N. Nakanishi and I. Ojima, *Covariant Operator Formalism of Gauge Theories and Quantum Gravity* (World Scientific, 1990).

[44] V. N. Gribov, "Quantization of non-Abelian gauge theories", *Nuclear Physics B*, vol. 139, p. 1, 1978.

[45] I. M. Singer, "Some Remarks on the Gribov Ambiguity", *Communications in Mathematical Physics*, vol. 60, p. 7, 1978.

[46] N. Vandersickel and D. Zwanziger, "The Gribov problem and QCD dynamics", *Physics Reports*, vol. 520, p. 175, 2012, arXiv:1202.1491 [hep-th].

[47] G. Jona-Lasinio, "Relativistic Field Theories with Symmetry-Breaking Solutions", *Il Nuovo Cimento (1955-1965)*, vol. 34, p. 1790, 1964.

[48] G. t' Hooft and M. Veltman, "Regularization and renormalization of gauge fields", *Nuclear Physics B*, vol. 44, p. 189, 1972.

[49] L. Baulieu and J. Thierry-Mieg, "The principle of BRS symmetry: An alternative approach to Yang-Mills theories", *Nuclear Physics B*, vol. 197, p. 477, 1982.

[50] A. A. Slavnov, "Ward identities in gauge theories", *Theoretical and Mathematical Physics*, vol. 10, p. 99, 1972.

[51] J. C. Taylor, "Ward identities and charge renormalization of the Yang-Mills field", *Nuclear Physics B*, vol. 33, p. 436, 1971.

[52] T. Matsubara, "A New Approach to Quantum-Statistical Mechanics", *Progress of Theoretical Physics*, vol. 14, p. 351, 1955.

[53] C. D. Roberts and A. G. Williams, "Dyson-Schwinger Equations and their Application to Hadronic Physics", *Progress in Particle and Nuclear Physics*, vol. 33, p. 477, 1994, arXiv:hep-ph/9403224.

[54] C. D. Roberts and S. M. Schmidt, "Dyson-Schwinger equations: Density, temperature and continuum strong QCD", *Progress in Particle and Nuclear Physics*, vol. 45, p. S1, 2000, arXiv:nucl-th/0005064.

[55] R. Alkofer and L. von Smekal, "The infrared behaviour of QCD Green's functions: Confinement, dynamical symmetry breaking, and hadrons as relativistic bound states", *Physics Reports*, vol. 353, p. 281, 2001, arXiv:hep-ph/0007355.

[56] P. Maris and C. D. Roberts, "Dyson–Schwinger Equations: A Tool for Hadron Physics", *International Journal of Modern Physics E*, vol. 12, p. 297, 2003, arXiv:nucl-th/0301049.

[57] C. S. Fischer, "Infrared properties of QCD from Dyson–Schwinger equations", *Journal of Physics G*, vol. 32, p. R253, 2006, arXiv:hep-ph/0605173.

[58] R. Alkofer, C. S. Fischer, F. J. Llanes-Estrada, and K. Schwenzer, "The quark–gluon vertex in Landau gauge QCD: Its role in dynamical chiral symmetry breaking and quark confinement", *Annals of Physics*, vol. 324, p. 106, 2009, arXiv:0804.3042 [hep-ph].

[59] A. C. Aguilar, D. Binosi, J. C. Cardona, and J. Papavassiliou, "Nonperturbative results on the quark-gluon vertex", in proceedings of "Xth Quark Confinement and the Hadron Spectrum", *PoS(Confinement X)103* (2012), arXiv:1301.4057 [hep-ph].

[60] E. Rojas et al., "On the quark-gluon vertex and quark-ghost kernel: combining lattice simulations with Dyson-Schwinger equations", *Journal of High Energy Physics*, vol. 2013, issue 10, no. 193, p. 1, 2013, arXiv:1306.3022 [hep-ph].

[61] S.-X. Qin et al., "Interaction model for the gap equation", *Physical Review C*, vol. 84, p. 042202–1, 2011, arXiv:1108.0603 [nucl-th].

[62] K. A. Olive et al. (Particle Data Group), "Review of Particle Physics", *Chinese Physics C*, vol. 38, p. 090001, 2014.

[63] J. Stoer and R. Bulirsch, *Introduction to Numerical Analysis* (Springer New York, 2002).

[64] W. Gautschi, *Numerical Analysis* (Birkhäuser Basel, 2012).

[65] M. Abramowitz and I. A. Stegun, eds., *Handbook of Mathematical Functions with Formulas, Graphs, and Mathematical Tables* (Dover Publications, 1965).

[66] K. Raya et al., "Multiple solutions for the fermion mass function in QED3", *Physical Review D*, vol. 88, p. 096003–1, 2013, arXiv:1305.2955 [nucl-th].

[67] W. Celmaster and R. J. Gonsalves, "Quantum-Chromodynamics Perturbation Expansions in a Coupling Constant Renormalized by Momentum-Space Subtraction", *Physical Review Letters*, vol. 42, p. 1435, 1979.

[68] W. Celmaster and R. J. Gonsalves, "Renormalization-prescription dependence of the quantum-chromodynamic coupling constant", *Physical Review D*, vol. 20, p. 1420, 1979.

[69] J. I. Skullerud and A. G. Williams, "The Quark Propagator in Momentum Space", *Nuclear Physics B (Proceedings Supplement)*, Proceedings of the XVIIth International Symposium on Lattice Field Theory, p. 209, 2000, arXiv:hep-lat/9909142.

[70] M. Schröck, "The chirally improved quark propagator and restoration of chiral symmetry", *Physics Letters B*, p. 217, 2012, arXiv:1112.5107 [hep-lat].

[71] M. Le Bellac, *Thermal Field Theory* (Cambridge University Press, 1996).

[72] J. A. Müller, "A Dyson–Schwinger Approach to Finite Temperature QCD", PhD thesis (Technische Universität Darmstadt, 2011).

[73] A. Bender, D. Blaschke, Y. Kalinovsky, and C. D. Roberts, "Continuum Study of Deconfinement at Finite Temperature", *Physical Review Letters*, vol. 77, p. 3724, 1996, arXiv:nucl-th/9606006.

[74] A. Bazavov et al. (HotQCD Collaboration), "Chiral and deconfinement aspects of the QCD transition", *Physical Review D*, vol. 85, p. 054503–1, 2012, arXiv:1111.1710 [hep-lat].

[75] C. A. Welzbacher, "Quarks and Gluons in the Phase Diagram of Quantum Chromodynamics", PhD thesis (Justus-Liebig-Universität Gießen, 2016).

[76] C. S. Fischer, private communication, 2017.

[77] J. M. Cornwall, R. Jackiw, and E. Tomboulis, "Effective action for composite operators", *Physical Review D*, vol. 10, p. 2428, 1974.

[78] R. W. Haymaker, "Variational Methods for Composite Operators", *La Rivista del Nuovo Cimento*, vol. 14, p. 1, 1991.

[79] D. Müller, "QCD at finite density with Dyson–Schwinger equations", PhD thesis (Technische Universität Darmstadt, 2013).

[80] C. R. Allton et al., "Thermodynamics of two flavor QCD to sixth order in quark chemical potential", *Physical Review D*, vol. 71, p. 054508–1, 2005, arXiv:hep-lat/0501030.

[81] W. Greiner and J. Reinhardt, *Field Quantization* (Springer Berlin Heidelberg, 1996).

Erklärung zur Master-Arbeit

Hiermit versichere ich, die vorliegende Master-Arbeit ohne Hilfe Dritter nur mit den angegebenen Quellen und Hilfsmitteln angefertigt zu haben. Alle Stellen, die aus Quellen entnommen wurden, sind als solche kenntlich gemacht.

Darmstadt, den 22. Februar 2017

(Philipp Isserstedt)